ABSTRACT

HUNT-LOWERY, ALISA. Statistical Analysis of Novel Dielectric Materials for Microelectronics. (Under the direction of Yahya Fathi and Jon-Paul Maria.)

This research analyzes the re-oxidation annealing process of Barium titanate thin films on copper foils made by Chemical Solution Deposition. During this anneal, the temperature and oxygen pressure settings must be optimized to ensure the elimination of oxygen vacancies without oxidizing the copper foil substrate. This research utilizes Design of Experiments (DOE) to study the impact of re-oxidation furnace temperature and pressure on the dielectric loss tangent response. Two designs of experiments were run. The first experiment, a 3^2 DOE, examined a large range of temperature and pressure levels. Due to the high susceptibility of uncontrollable factors such as humidity and film position in the crystallization anneal furnace, an adequate model could not be developed. However, the temperature at 550ºC and a pressure of 10^{-5} Torr yielded a lower mean and standard deviation of the loss tangent response. A second and smaller scale experiment, a 2^2 with a center point, was run around 550ºC and 10^{-5} Torr to determine if more optimal temperature and pressure settings existed in the local area. Two second order response surface models were developed from two crystallization anneals that were statistically significant. The most significant finding was that the optimum level for temperature and pressure in the re-oxidation anneal furnace in this experiment is 550ºC and $2x10^{-5}$ Torr. While the models concluded that the temperature, pressure, temperature quadratic, and interaction between pressure and temperature were important effects in the model, there were differences in the curvature of the models due to the temperature quadratic effect.

STATISTICAL ANALYSIS OF NOVEL DIELECTRIC MATERIALS FOR MICROELECTRONICS

by

ALISA HUNT-LOWERY

A thesis submitted to the Graduate Faculty of
North Carolina State University
in partial fulfillment of the
requirements for the Degree of
Master of Science

INDUSTRIAL ENGINEERING

Raleigh

2004

Co-Chair of Advisory Committee

Co-Chair of Advisory Committee

DEDICATION

To my parents, James and Alice.

BIOGRAPHY

Alisa Hunt was born on June 22, 1976, in Laurinburg, NC to James Edward and Alice Wynne Hunt of Rowland, NC. She is the third of four children. She graduated from Purnell Swett High School in 1994 as the valedictorian. She attended North Carolina State University and graduated magna cum laude in textile engineering in May 1998. After graduation, she worked as a production manager and process engineer with Milliken & Co. in Blacksburg, SC. She left Milliken & Co. in August 1999 to marry her college sweetheart, Robin R. Lowery of Pembroke, NC, whom she met while at NC State. She then took a job with the NC State University College of Engineering Office of Minority Engineering Programs where she worked as Assistant Director until she came back to school full time as a graduate student in industrial engineering in August 2002. Alisa received a Masters Scholarship from the Semiconductor Research Corporation (SRC) to pursue her master's studies. She worked with Jon-Paul Maria's Center for Electroceramic Thin Films as a research assistant to optimize dieletric thin film processes, specifically for the re-oxidation anneal.

ACKNOWLEDGEMENTS

I would like to thank my committee co-chairs: Dr. Yayha Fathi for your theoretical discussions and guidance through out my research even though his own background was so varied from my research and Dr. Jon-Paul Maria who agreed to take on such an unorthodox student and from outside his own discipline. I would also like to thank Dr. John Hren and Dr. Victor Zhirnov, both who were very instrumental in helping me find SRC and a sponsoring faculty member. I would also like to thank Dr. Tom Johnson, whose statistics classes and discussions I enjoyed and introduced me to JMP. I would also like to thank Dr. Jim Wilson, a committee member. Thanks to Jon Ihlefeld who has tutored me in kinetics and crystal chemistry and made all the samples that I used in my research and to the rest of my research group who have assisted me.

Personally, I would like to thank my parents, James and Alice Hunt, who made tremendous personal and financial sacrifices through out the years for my education and simply because I wanted so much. My parents' dedications to family, to God and uncompromising work ethic have all been my inspiration. I also want to thank my siblings, Sherry, Timothy, and Jamie, for being so understanding when Daddy and Mama made so many concessions for my education. I would also like to acknowledge my grandmothers, Mary Brewer Woods Wynne, and Della Hunt, both of whom I lost while working on my master's degree in 2003. I have numerous other extended family members who have been supportive of my education through out the years, "Thank you." Finally, I would like to thank Rod, my husband, who has been my rock and confidant throughout my college experiences. His wisdom and guidance has kept me sane and grounded throughout my educational experience and in life.

TABLE OF CONTENTS

LIST OF FIGURES

LIST OF TABLES

CHAPTER 1

INTRODUCTION

Moore's Law states that the transistor performance should be doubled and the number of devices on a chip should be quadrupled every four years [1]. Wang even suggests that the trend to produce smaller and smaller devices has far exceeded Moore's Law [2]. As integrated circuits are scaled, discrete components and packaging materials must also continue to scale at a rapid pace in order to maintain the International Technological Roadmap for Semiconductors (ITRS). Currently, discrete and passive components including capacitors are mounted on top of a polymer packaged printed wiring board (PWB) as surface mounted multi-layer capacitors (MLCs).

MLCs are made using a bulk ceramic material with base metal electrodes (BME). They have high capacitance and a small size, high reliability, and high frequency characteristics [3]. This bulk ceramic is stacked hundreds of layers thick to create a high capacitance, multi-layer ceramic capacitor (MLC), see Figure 1.1 [3].

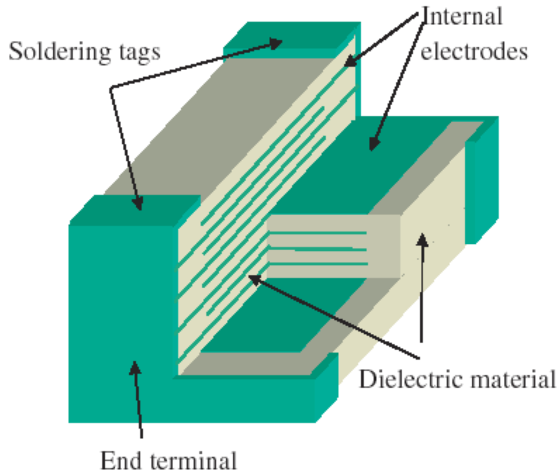

Figure 1.1: Multi-layer Ceramic Capacitor [3]

If these capacitors work so well, why replace them? The Internet boom of the mid 90s compelled the microelectronics world to create devices that would function better with less space. As long as technological advances are made with continuous high reliability, consumers will continue to buy the best technology with faster speed. Over three billion MLCs are used in the US each year [4]. However, passive components contribute the largest single number of failures of electronic components, see Figure 1.2 [5].

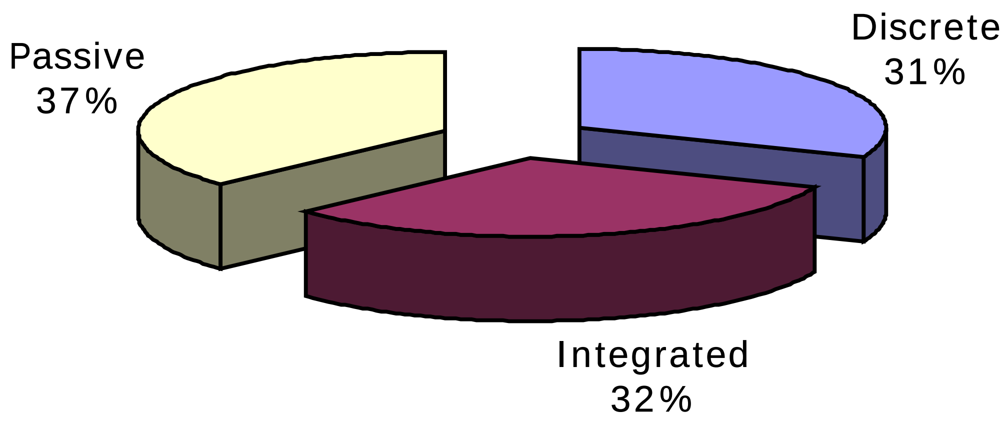

Figure 1.2: Electronic failures by component [6]

This research involves eliminating the surface mounted capacitors and replacing them with a planar thin film that will be embedded on the interior of a printed wiring board, thus reducing the packaging and allowing for greater integration density. Surface space is freed as capacitors and interconnects are moved to within the PWB, offering additional board area for integrated circuits (ICs) and other active devices. Device reliability increases due to fewer soldered connections between chips, capacitors, and interconnects, and the ability to locate devices directly above decoupling capacitors shortens interconnect lengths. This in turn decreases the lead inductance and increases the maximum frequency of operation [7,8].

Barium Titanate ($BaTiO_3$) is used to make the film because of its frequency performance, high intrinsic dielectric constant, high resistance to temperature and humidity, and economic integration with high volume production manufacturing [4]. The films are prepared by chemical solution and deposited on a rough copper foil, a much less expensive alternative to current substrates of platinum deposited on smooth silicon. They are then fired in a reducing atmosphere at high temperatures. A subsequent anneal, or re-oxidation anneal, at a lower temperature and higher partial oxygen pressure is performed to minimize the number of oxygen vacancies that make the film electrically unreliable.

This thesis analyzes the re-oxidation annealing process parameters utilizing Design of Experiments and Response Surface Analysis to increase the electrical reliability of the film. Design of Experiments (DOE) uses statistics to assist in making valid and objective conclusions about a process or system. DOE is used because it is a cost-effective process improvement methodology that allows the researcher to make simultaneous changes to the system while discovering what parameter levels improve the system.

The remaining chapters of this thesis are organized as follows. In Chapter 2, we present a literature review. In Chapter 3, we present the results of the initial experiments and related statistical analysis. In Chapter 4, we present the results of a second (and final) experiment. Finally, Chapter 5 contains some concluding remarks.

CHAPTER 2

LITERATURE REVIEW

This study applies statistical tools (Designs of Experiments) to improve a microelectronic material's kinetics process. DOE uses statistics to assist in making valid and objective conclusions about a process or system [23]. However, before we begin our statistical analysis, we must first understand the dielectric's properties. This chapter discusses dielectric properties, provides an overview of dielectric breakdown, and presents statistical methods used in this research. Dielectric breakdown is presented by first introducing defects in silicon oxide (SiO_2) materials since these mechanisms can be deployed to dielectric breakdown. Then perovskite failure modes applied to dielectrics are discussed. The film deposition technology is presented. The chapter concludes with a review of the steps used in Design of Experiments.

2.1 Current Multi-Layer Ceramic Capacitors

Multi-layer Ceramic Capacitors are formulated to obtain particular characteristics. The three main capacitors are NPO or COG, X7R, Z5U, and Y5V, see Table 2.1 [3]. Typically as the dielectric constant, κ, increases, the capacitor is less stable in relation to temperature. Capacitors are grouped by classes. Class 1 includes the NPO/COG capacitors which are highly stable when under heat, voltage, and frequency. These are the most reliable capacitors according to military standards. These capacitors exhibit more paraelectric (not ferroelectric) behavior, and electrical characteristics are less dependent on voltage, temperature, and frequency. X7R are the general purpose capacitors, but are only semi-stable and reside in Class 2. The films used in this research are comparable to the properties of X7R MLCs. Z5U and Y5V are less stable and their characteristics are more temperature, frequency, and voltage dependent. Z5U and Y5V are Class 2 capacitors. Class 2 capacitors are less stable, but have higher capacitance values [9].

Table 2.1: Multi-layer ceramic capacitor characteristics [3]

TYPE	κ Value	$BaTiO_3$ content (%)	Other Dopants	Capacitance Range	Grain size (μm)	Temp. Range	Temp.-Capac. Change
COG/ NPO	100	10-50	TiO_2, $CaTiO_3$, $Nd_2Ti_2O_7$	1pF-1nF	1	-55 to 125 °C	0±30ppm/°C
X7R	4,000	90-98	MgO, MnO, Nb_2O_5, CoO, Rare Earth	10nF-100nF	<1.5	-55 to 125 °C	0±15%
Y5V	18,000	80-90	$CaZrO_3$, $BaZrO_3$	100nF-1000nF	3-10	-30 to 85°C	+22%, -82%
Z5U	14,000	80-90	$CaZrO_3$, $BaZrO_3$	100nF-1000nF	3-10	+10 to 85°C	+22%, -56%

2.2 Dielectric Properties

2.2.1 Capacitance

An important characteristic of dielectric films is capacitance. Capacitance is defined as:

$$C = \frac{\varepsilon_o \varepsilon_R A}{t} \qquad (2.1)$$

where ε_o is the relative permittivity of free space, $8.85 \cdot 10^{-14}$ F/cm, and ε_R is the permittivity of the material [10]. *A* is the area of the film and *t* is the thickness of the capacitor. Therefore the capacitance is a function of the material, but also of the geometry of the device. This is why the dielectric constant, κ, is more often used to describe dielectric properties.

$$\kappa = \frac{\varepsilon_R}{\varepsilon_o} \qquad (2.2)$$

The dielectric constant, κ, is independent of the film's thickness. A thin film with a higher dielectric constant is desired when making capacitor devices.

2.2.2 Loss Tangent

Since every capacitor is not created the same, the loss tangent can be used to characterize the dielectric material. The loss tangent can change with each capacitor and may be independent of the processing conditions. The loss tangent gives us insight to the dielectric performance via energy loss[11]. Loss tangent is measured as a percent, and a lower loss tangent yields a better capacitor. Loss tangent is a ratio of resistance to capacitive reactance, X_C, which is the effect of capacitance and frequency [9]. Or it can be restated that loss tangent is a ratio of real, *R*, and imaginary components, X_C, of resistance that can be used to determine capacitor quality.

$$Loss\ Tangent = \frac{R}{X_C} = 2\pi fCR \ [9] \qquad (2.3)$$

where $X_C = \dfrac{1}{2\pi fC}$ is the capacitive reactance, and f is the frequency of the test signal, which may vary from 5Hz to 13MHz. The loss tangent is also used to measure the efficiency of the capacitor [11]. The "Q" or quality factor is the reciprocal of loss tangent and is sometimes used to describe the dielectric's characteristics.

2.3 Chemical Solution Deposition Barium Titanate Thin Films

Chemical Solution Deposition (CSD) refers to the deposition method of creating a dielectric using a multi-component chemical solution containing barium and titanium ions. This solution can be deposited on a variety of substrates, including base metal electrodes made from nickel, platinum, other precious metals, and ceramics. Barium Titanate ($BaTiO_3$) is a ceramic material with a perovskite crystal structure that displays ferroelectric properties. The crystal structure of this compound is shown in Figure 2.1. A perovskite compound (ABO_3) consists of an alkaline earth metal (denoted by A), a transition metal (denoted by B) and oxygen to form the oxide (denoted by O).

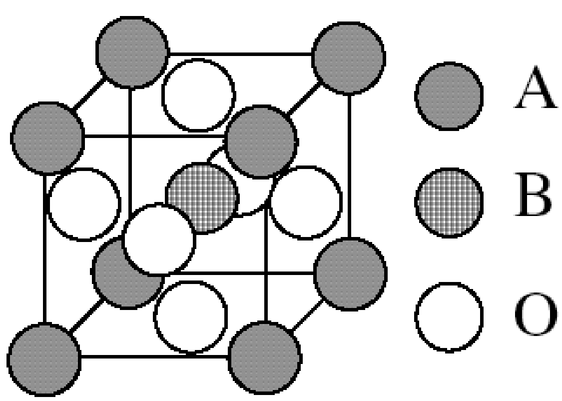

Figure 2.1: Perovskite Crystal Structure [12]

The as processed films are polycrystalline, dense, and exhibit an equiaxed (spherical-like) morphology with an average grain size of 140 nm [13]. The microstructure of these films greatly influences their electronic properties including: capacitance-voltage, capacitance-frequency, and loss tangent. Each processing step is critical to create a robust, high-yield and highly reliable film. This thesis focuses on the annealing process, particularly the second anneal or re-oxidation anneal.

2.3.1 CSD $BaTiO_3$ Annealing Processes

There are four main processing steps in making CSD $BaTiO_3$ thin films with Copper base metal electrodes (BME):

1. Deposit $BaTiO_3$ solution on rough Cu foil
2. Fire in Reducing Atmosphere: Crystallization Anneal
3. Fire in re-oxygenating atmosphere: Re-oxidation anneal
4. Deposit platinum electrodes

This thesis focuses on the annealing step, particularly the re-oxidation anneal. However, both the crystallization and re-oxidation anneal are discussed in this literature review. The crystallization anneal is performed in a reducing atmosphere of N_2 and H_2 at high temperatures to crystallize the film and to oxidize the barium and titanium to form barium titanate ($BaTiO_3$) while preventing copper from oxidizing. For copper substrates, this is done at 900°C and 10^{-11} atm of partial pressure of oxygen (pO_2). N_2 with its low level of impurities (O_2, C, etc…) combined with a small amount of H_2 is used to create H_2O; this allows a low pO_2 to be achieved [13]. However, at the end of this process, the barium and titanium solution is not completely oxidized; the compound is actually $BaTiO_{3-x}$, where x is the number of oxygen vacancies. Therefore another anneal or the re-oxidation anneal must be done to continue to oxidize the barium and titanium and reduce the number of oxygen vacancies, since each oxygen vacancy produces two electrons (charge 2^-). These two electrons increase the conductivity of the dielectric, making it susceptible to electronic degradation [14]. The re-oxidation or replacing of oxygen into the dielectric to fill the oxygen vacancies, eliminates the electrons and increases the electrical stability of the capacitor. This is done at higher pressure (~1-50ppm of O_2) and lower temperatures (450°C-650°C) to decrease the possibility of the copper oxidizing [15]. The re-oxidation anneal increases the lifetime of BME capacitors by a factor of 10 and increases the insulation resistance of the dielectric [15]. In addition, the film on the copper foil is now dense, preventing O_2 from penetrating and oxidizing the foil. Therefore, this re-oxidation anneal is a critical step in creating the $BaTiO_3$ thin films and is the focus of this research.

2.4 Dielectric Breakdown

Dielectric breakdown can be categorized into two types of failures: extrinsic caused by mechanical defects and intrinsic defects, characterized by inherent defects in the film. Electrical properties are affected by intrinsic defects. These are analyzed in this thesis. Dielectric breakdown does not necessarily mean the film has experienced catastrophic failure, but that under some environmental stress, the material characteristics have changed. While there has been much research in the area of silicon dioxide (SiO_2) Metal Oxide Semiconductor (MOS) insulator failures, little research has analyzed failures from other types of thin films, particularly perovskite oxides with base metal electrodes that are used in MLCs. Therefore, SiO_2 failures are reviewed and then perovskite failure modes.

2.4.1 SiO_2 Extrinsic Defects

Extrinsic defects occur as a result of device fabrication or processing. Extrinsic defects are often a result of mechanical failures or occur during fabrication. Examples are pinholes or scratches on the surface of the film that result in an electrical short. Other examples are contaminants, moisture, and metallic migrations [16]. These defects occur at low electric fields (1-2MV/cm) applied for short periods of time. These are often referred to as “A” mode defects in silicon. These may be defects that are detected during the “burn in” of microelectronic components. Therefore, it is critical to burn in devices to screen for marginal performance [17]. Shorter testing times at higher voltages will lower the failure rate for the surviving capacitors [18].

2.4.2 SiO_2 Intrinsic Defects

Intrinsic defects characterize the film’s materials properties. These defects may result in dielectric failure. Factors that may affect intrinsic breakdown are doping, grain size, stoichiometry, second phases, porosity and electrode properties [19]. There are four categories of dielectric failure: time dependent dielectric breakdown, TDDB; noisy or “soft” breakdown; resistance degradation; and stress induced leakage current (SILC) [12]. Schroeder says these occur at higher electrical fields and take longer to breakdown. These are also known as “C” mode defects in silicon [17].

2.4.3 Perovskite Failure Modes

There has been much research of bulk ceramic Nickel (Ni) base metal electrode (BME) MLCs. Bulk ceramic failure modes may also be used to describe thin film failure modes [3]. Ni MLCs are doped to change the properties of the capacitor. The base metal electrodes also contribute to electrical degradation of the dielectric through conduction from the anode to the cathode via oxygen vacancies. As the insulation resistance (IR) of a capacitor degrades, the dielectric becomes thin and may break down, mainly seen in acceptor-doped materials [15]. According to Kishi, models discussing this breakdown include:

- Grain boundary model-Soft breakdown
- Reduction model-Time dependent dielectric breakdown
- De-Mixing-Oxygen vacancies

De-mixing of oxygen vacancies will not be discussed in this paper because this occurs mainly in doped materials.

2.4.3.1 Grain Boundary Model

Loh explains that DC leakage in barium titanate degradation is due to the Poole-Frenkel effect. Applying higher electric fields, $>10^5$ V/cm, in ferroelectric ceramic grains ionizes donors and traps in the grains adjacent to the grain surface. This ionization extends the electric polarization inward to the interior of the grain and eventually switches ferroelectric domains in the grain. The domain switching leads to a local dielectric breakdown [3]. In time dependent dielectric breakdown (TDDB), a leakage path is created between the electrodes by communicating electron traps, known as the percolation model in SiO_2, see Figure 2.2. The resistances of these paths are 10^2, 10^5, and 10^9 Ω for typical low voltage instable, "unreliable," and "normal" capacitors. Waser explains that the grain boundaries in ceramics exhibit higher specific resistivities than in bulk grains. After DC voltage is applied, Maxwell-Wagner polarization creates high electrical fields across the grain boundaries [19].

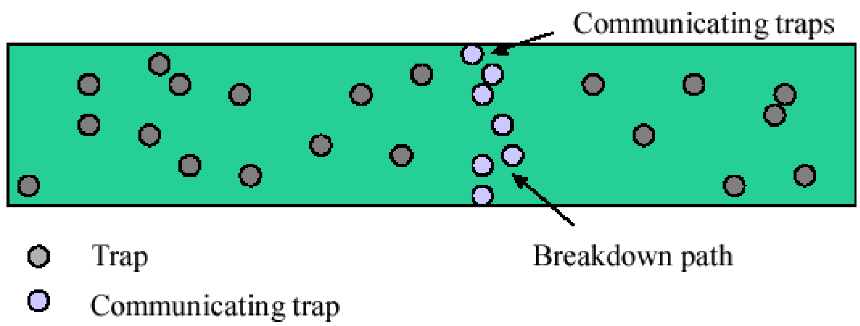

Figure 2.2: Percolation Model [20]

2.4.3.2 Reduction Model

Oxygen vacancies are formed during the annealing process after deposition. Oxygen vacancies have been explained by Lehovec as:

- High conductivity region spreads from cathode (bottom electrode-ground) to the anode (top electrode)
- Transport phenomena of electrons from the low conductivity region of anode (top electrode) to the cathode (bottom electrode-ground) after an electric field has been applied.

The high conductivity model explained the reduction model. After an electric field is applied, electrons are injected into the barium titanate, increasing the concentration of electrons. This causes a buildup of a negative space charge, thus reducing the field at the cathode [21]. This model is also known as time dependent dielectric breakdown because of the degradation of the insulation resistance of the dielectric. For the low conductivity process, if oxygen vacancies can be reduced or eliminated by either re-oxidation or by applying an electric field, this creates a high resistivity zone within the dielectric, preventing insulation resistance degradation [21].

2.5 Statistical Analysis

Statistical analysis is tool that can be applied to any process to discover trends, model data, and find data that do not fit any patterns [22]. Statistics is a set of tools that can be used to find out meaningful information about a process. This can be an industrial process, in the health care field, in a service industry, or any other process that involves the exchange of information. Not only is statistics a method of analyzing data, it can be used to improve a process. Design of Experiments is a statistical method employed in this research to analyze a kinetic process.

2.5.1 Design of Experiments

Design of Experiments involves planning experiments in order to draw meaningful conclusions from the data. Once the data are collected, then statistical analysis can be performed on the data [23]. Often in Design of Experiments, there is more than one person involved in these experiments and analysis. It often involves a team of people who have different expertise to contribute to the process. In this project, the team consists of four individuals, two people with process and materials chemistry experience and two individuals with statistical analysis experience. In order for all four to understand how to best utilize Design of Experiments, there are guidelines that can be followed to assist the team in understanding the overall goals of the project. According to Montgomery, there are seven guidelines for designing and analyzing an experiment:

1. Recognition and statement of the problem.
2. Choice of factors, levels, and ranges.
3. Selection of the response variable(s)
4. Choice of experimental design.

5. Performing the experiment.

6. Statistical analysis of the data.

7. Conclusions and recommendations.

Steps 1-4 are performed in a design process, before any data are gathered. Steps 5-7 are performed after the experiment is run. These 7 steps were used in completing this research.

CHAPTER 3

FIRST EXPERIMENT WITH THE RE-OXIDATION ANNEAL: A 3^2 DESIGN OF EXPERIMENT

In process optimization, Design of Experiments is often the natural statistical tool to use to optimize the response. Responses may include yield, distance, capacitance, yes/no data or any other discrete, continuous, or attribute data. Critical process parameters or factors are chosen that affect the responses. To locate the optimum, it is necessary to change the factors and run an experiment to determine which level(s) of each factor optimize the response.

3.1 Statement of the Problem

A new Chemical Solution Deposition process to make embedded thin film capacitors was created at North Carolina State University. This is a four step process discussed in the previous chapter:

1. Deposit $BaTiO_3$ solution on rough Cu foil
2. Fire in Reducing Atmosphere: Crystallization Anneal
3. Fire in re-oxygenating atmosphere: Re-oxidation anneal
4. Deposit platinum electrodes

During the first anneal, the $BaTiO_3$ crystalline structure is formed and the film is fired in a reducing atmosphere to prevent the copper foil from oxidizing [24]. However, at this point, the film is a poor insulator and poor conductor due to excess oxygen vacancies and electrons. Each oxygen vacancy creates two electrons, causing the film to act as a conductor. Therefore, the second anneal fills many of the oxygen vacancies to create properties more desired in a dielectric. However, during this second anneal, the temperature and pressure levels must be optimized to make sure most of the oxygen vacancies are filled with oxygen without oxidizing the copper film. If too much oxygen is added, then oxygen will search for vacancies in the copper substrate below the film, forming Copper (I) Oxide, which should never occur. If Copper (I) Oxide is formed below the film, this essentially creates two capacitors, C_{BaTiO_3} and C_{Cu_2O}. According to the following equation:

$$\frac{1}{C_{Total}} = \frac{1}{C_{BaTiO_3}} + \frac{1}{C_{Cu_2O}} \tag{3.1}$$

The total capacitance would then decrease. Therefore, the oxidation of copper must be prevented while optimizing annealing conditions to reduce oxygen vacancies.

3.2 Factors and Levels

The re-oxidation or second anneal has been identified as a critical step in the process. Three factors influence this step: time, temperature, and pressure. This step is very important in determining the quality and reliability of the capacitor. The two factors that were chosen were temperature and pressure. The initial operating set points for the re-oxidation anneal were 550°C and 10^{-5} Torr. The levels that were chosen for temperature were 450°C, 550°C, and 650°C. The levels that were chosen for pressure were: 10^{-5} Torr, 10^{-4} Torr, and 10^{-3} Torr, see Table 3.1. A full factorial experiment is performed to examine the effects of temperature, pressure, and the interaction between the two factors. The partial pressure of oxygen (pO_2) in the furnace and temperature (T) of the furnace are linearly related due to the oxygen vacancy concentration $[V_o^{\bullet\bullet}]$ of barium titanate according to the equation:

$$[V_o^{\bullet\bullet}] = \left[\frac{1}{4} pO_2^{-\frac{1}{2}} \exp\left(\frac{-\Delta H}{RT}\right)\right]^{\frac{1}{3}} \qquad (3.2)$$

[13,25]. Due to this relationship, temperature and log(pressure) are linearly related to the responses, thus the logarithmic scale for pressure is used. Thus, 10^{-5}, 10^{-4}, and 10^{-3} pressures are all equidistance on the linear scale. In this research, $\log(10^{-5})=-5$, or 0.00001, or 10^{-5}. These data formats are all used interchangeably to describe the partial pressure of oxygen levels.

Table 3.1: 3^2 Full Factorial Experiment: Factors and Levels

Factors	Levels
Temperature (°C)	450, 550, 650
Pressure (Torr)	10^{-5}, 10^{-4}, 10^{-3}

3.2.1 Controllable vs. Uncontrollable Factors

In each experiment, there are controllable factors of interest, such as the temperature and pressure of the furnace. Other factors are controllable, but are not of interest. These are called blocking factors and are discussed in Chapter 4. There are also uncontrollable factors, such as environment. Uncontrollable factors identified in this experiment are:

- Humidity that affects the yield and loss tangent
- Consistency of chemicals used to make barium titanate solution
- Film thickness uniformity
- Surface of Copper foils

Although the experimenter is aware of the uncontrollable factors, steps are taken to minimize their effects as much as possible by:

- Using the same chemicals for each designed experiment
- Spinning samples in a humidity controlled environment at 13% Relative Humidity
- Spinning at a constant rpm for the same amount of time for each layer
- Cleaning Copper foils consistently before use

3.3 Responses

This process involves finding out if a relationship exists between temperature and pressure of the re-oxidation anneal furnace on capacitance and loss tangent:

Loss Tangent = f(Temperature, Pressure)

Capacitance = g(Temperature, Pressure)

The responses used in these experiments were loss tangent and capacitance at 0 Volts. These measurements are very susceptible to human error because the voltage is manually turned on and off and the measurements are taken by manually writing down the capacitance and loss tangent values. Therefore, it was essential to perform a Measurement System Analysis or Gauge R&R study, see section 3.3.1. Minimizing loss tangent was the primary goal of this project because this is more critical for capacitor efficiency. Maximizing capacitance was a goal, but the loss tangent response is a significant indicator of how effective the re-oxidation anneal is in completely oxidizing the barium and titanium. The average and standard deviation of these responses were measured as well. However, before measurements were taken, a Measurement System Analysis or Gauge Repeatability and Reproducibility study was performed to see if the measurement system is reliable.

3.3.1 Measurement System Analysis

Measurement system analysis (MSA) should be performed before collecting any data to confirm confidence in the measurement system. A MSA is a designed experiment to determine the reliability of the measurement system [23]. For variable or continuous data, the measurement system includes the units measured, three operators, and the gauge or equipment. When a unit is measured, the total variability in the measurement represents the part-to-part or product variation, the repeatability of the gauge, and the reproducibility of the operator, see Figure 3.1 and equation 3.4.

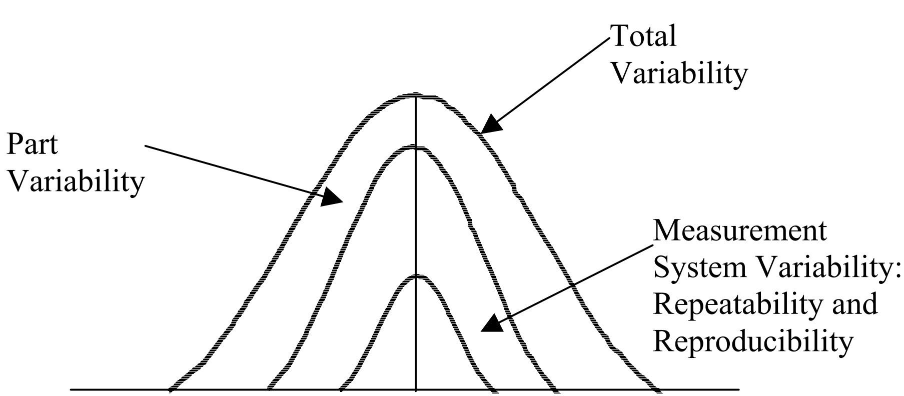

Figure 3.1: Total Variation in a Process [26]

Measurement System Variability=Repeatability + Reproducibility

$$\sigma^2_{\text{Measurement System}} = \sigma^2_{\text{Repeatability}} + \sigma^2_{\text{Reproducibility}} \tag{3.3}$$

The variance components of this system is:

$$\sigma^2_{Total} = \underbrace{\sigma^2_{Part}}_{\text{Part}} + \underbrace{\sigma^2_{Operator} + \sigma^2_{Part*Operator}}_{\text{Reproducibility}} + \underbrace{\sigma^2_{Error}}_{\text{Repeatability}} \tag{3.4}$$

Reproducibility is defined as the degree of agreement when multiple operators to measure the same part [26]. This is also referred to as the variation of the operators and the variation of the interaction between operators and parts [23]. Repeatability is the variation when the same operator measures the same part. This is often called the within or error variation from the gauge.

A crossed Gage Repeatability & Reproducibility Study was performed in this research to measure the loss tangent response since that is the response used in this research. A crossed study is when the same part is measured multiple times by three operators. It uses the two factor factorial with random effects to estimate the variance components from the operator, part, and interaction of operator and parts [23]. The variance components are estimated using the Analysis of Variance (ANOVA) method. ANOVA uses sum of squares, and mean squares to estimate the variance, see Table 3.2 [23].

Three operators measure 10 capacitors twice (3x10x2=60 observations) using the same measurement device. To examine the data from this experiment, see Appendix A. See Figure 3.2 for a schematic of the sampling plan.

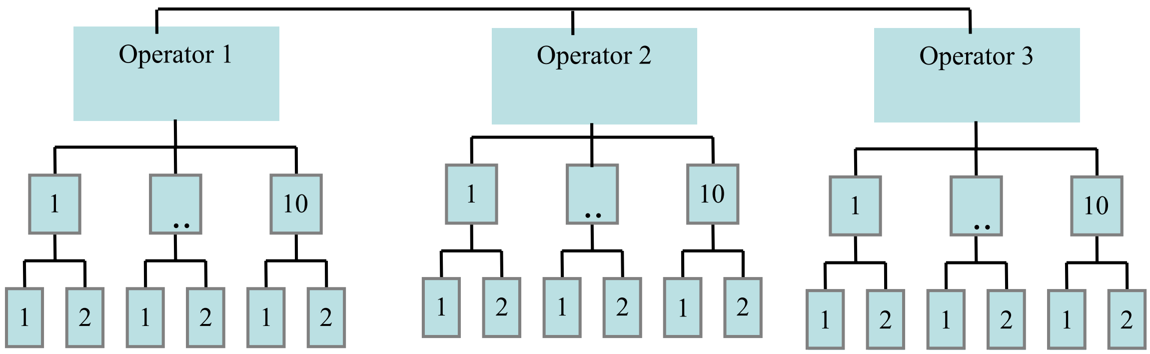

Figure 3.2: Sampling Plan for MSA[26]

In order to be confident the measurement system is reliable, the part-to-part variation should comprise 90% of the total variation [26]. The variation from the gauge and the operator should only comprise 10% of the variation. JMP SAS statistical software was used to analyze the data. Figure 3.3 shows the loss tangent variability chart by operator. The 650, 1E-4 capacitor seemed to have the most variation from each operator. This may have been because the counting could have been subjective by each operator.

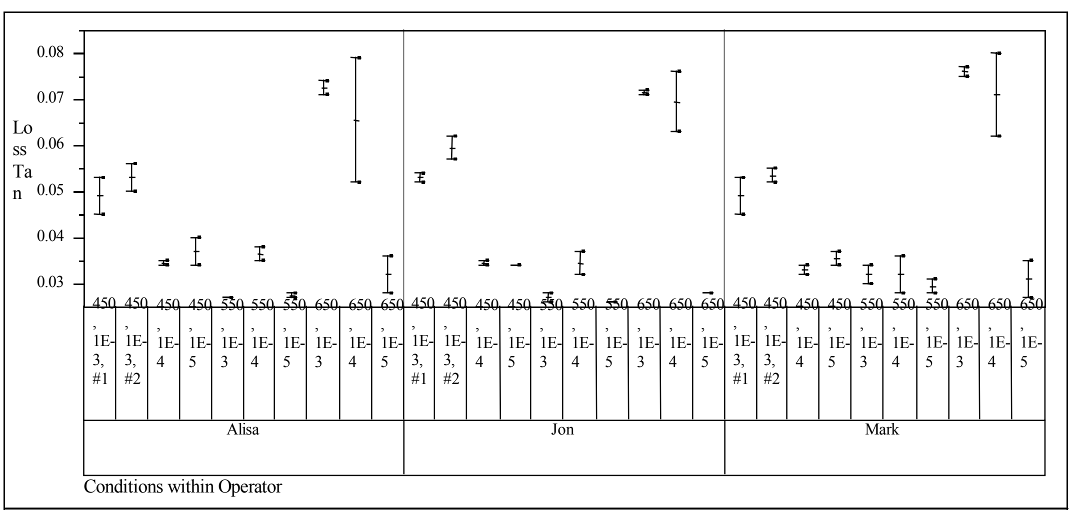

Figure 3.3: Loss Tangent Variability by Operator for each capacitor

Figure 3.4 shows the range of loss tangent values by operator. This chart shows that all the measured responses by the operators were within similar ranges. Figure 3.5 one shows the standard deviation of loss tangent by operator. The standard deviation by operators did not show any significant differences, indicating that the variations in procedures were minimal for each operator.

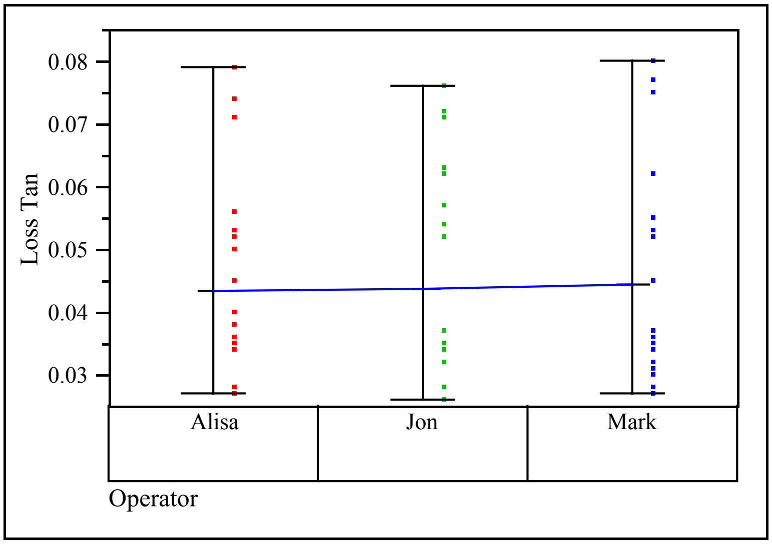

Figure 3.4: Range for Loss Tangent by Operator

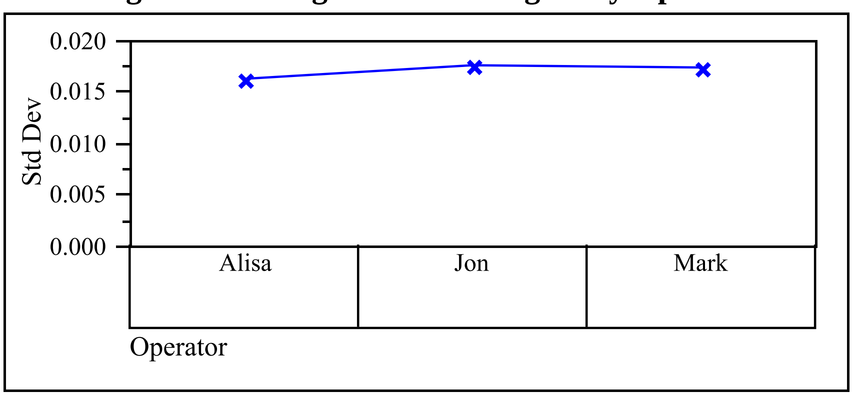

Figure 3.5: Standard Deviation for Loss Tangent by Operator

A drawback of using ANOVA to estimate the variance is sometimes negative variances are obtained. This can be dealt with several ways. JMP assumes the variance to be 0 if a negative variance is calculated. Another method to use is maximum likelihood estimates, but since the p-values of the variance components are large, there may not be an effect from the operator and interaction between operators and parts [23]. The 0 variance from these two effects makes sense because the operator is only placing the sample on the stage and then pressing a button for the gauge to measure the part and this is accomplished with little variation. The negaitive variances can also be explained as “garbage” put out by computers due to finite calculations.

Table 3.2: Analysis of Variance for Gauge R&R

Source	DF	SS	Mean Square	F Ratio	Prob > F
Operator	2	0.000007	3.27e-6	0.271	0.7658
Part	9	0.015549	0.00173	143.219	<.0001
Operator*Part	18	0.000217	0.00001	0.415	0.9733
Within	30	0.000873	0.00003		
Total	59	0.016645	0.00028		

Finally, Table 3.3 illustrates that 90.77% of the variation comes from part-to-part variation, and only 9.23% comes from the measurement system. The 9.23% variation in the measurement system comes from the repeatability or making multiple measurements. Since the measurement system variation is less than 10%, it can be concluded the measurement system is reliable and there is confidence that further investigation of the variation of the loss tangent response is not due to variation in the measurement system (operators or equipment).

Table 3.3: Variance Components for Gauge R&R

Component	Variance Component	% of Total	Plot%
Gage R&R	0.00002908	**9.23**	
Repeatability	0.00002908	**9.23**	
Reproducibility	0.00000000	**0.00**	
Part-to-Part	0.00028593	90.77	

3.4 Experimental Design

The purpose of this experiment is to create a baseline and to gather information. Therefore, as much information as possible must be ascertained from the experiments. A full factorial, two factor, three level (or a 3^2) experiment was run. At each treatment, we collected data for 40 capacitors. However, we chose all 40 capacitors from among the 108 capacitors deposited on one film. We did not use multiple films due to time and resources. For example, if we wanted 40 data points from each of the nine treatments, we would have to make 9*40=360 films. We also did not use a blocked design. Blocking was used in a subsequent experiment. There were many improvements that were implemented in the next experiment.

3.5 Performing the Experiment

Since this process involves optimizing an already existing process, the process of making the films is considered robust, and careful planning was involved before the experiment was ran. The experiment was performed by another group member and Ph.D. student who has the expertise in making chemical solution deposition thin films. The next section details the experimental procedure. After the film is deposited, the loss tangent and capacitance measurements are taken.

3.5.1 Experimental Procedure

A chemical solution deposition film is created using a precursor solution of barium and titanium atoms. The precursor solution is spun coated on 18 μm thick bare copper foils at 3000 rpm for thirty seconds. The film is then dried using a 250°C hot plate for 7 minutes. This process is repeated four times to create a film approximately 1 μm thick. The films are then crystallized in a reducing atmosphere at 900°C and ~pO_2 10^{-11} atm (0 Torr) in an atmospheric pressure controlled atmosphere furnace using H_2 and N_2 gases. Next, a re-oxidation anneal is performed in the same furnace under three different levels for pressure in Torr (10^{-5}, 10^{-4} and 10^{-3}) and three different levels of temperature in °C (450, 550, 650) to create a 3^2 full factorial design of experiment. Platinum electrodes that are 100 nm thick are then deposited on top of the film using DC magnetron sputtering through a shadow mask [13]. As mentioned earlier, the quality of the solution determines the yield of the capacitors. The film crystallinity and phase developments are studied using a Bruker AXS D-5000 x-ray diffractometer with a GADDS area detector. The x-ray diffraction pattern shows a "well-prepared ceramic material" compared to traditionally processed thin films [13]. Also, no Cu_2O or CuO phases are found in the film. If an oxide is created with the copper, the electrical reliability of the film could be diminished. Since the film grains and crystallinity have proved to be robust, electrical measurements were taken.

A HP 4192A Impedance Capacitance Resistance (LCR) Analyzer was used to measure the capacitance and loss tangent at a mid-range frequency of 10kHz and .05V oscillating voltage at 0 Volts of each capacitor at 25°C. This measurement is achieved by applying 3 Volts to the capacitor for 10 seconds to move all the dipoles in one direction so the capacitance value will be more accurate. Then the voltage is removed for 10 seconds and the capacitance and loss tangent measurements are taken. The film, approximately 1.5 cm x 1.5 cm, magnified 10X-60X times, is viewed using an Olympus SZ 60 microscope with a light source. See Figure 3.6 for a schematic of the film with deposited platinum electrodes. Columns 1-6, each has 18 oblong capacitors, yielding up to 108 capacitors. Capacitors were tested by column. Capacitors that were not shorted were tested in each column. On most films, 40 capacitors are tested, see Tables 3.4 and 3.5. Capacitors with a loss tangent value greater than 0.1 were excluded from this study. The capacitors were not chosen at random across the film.

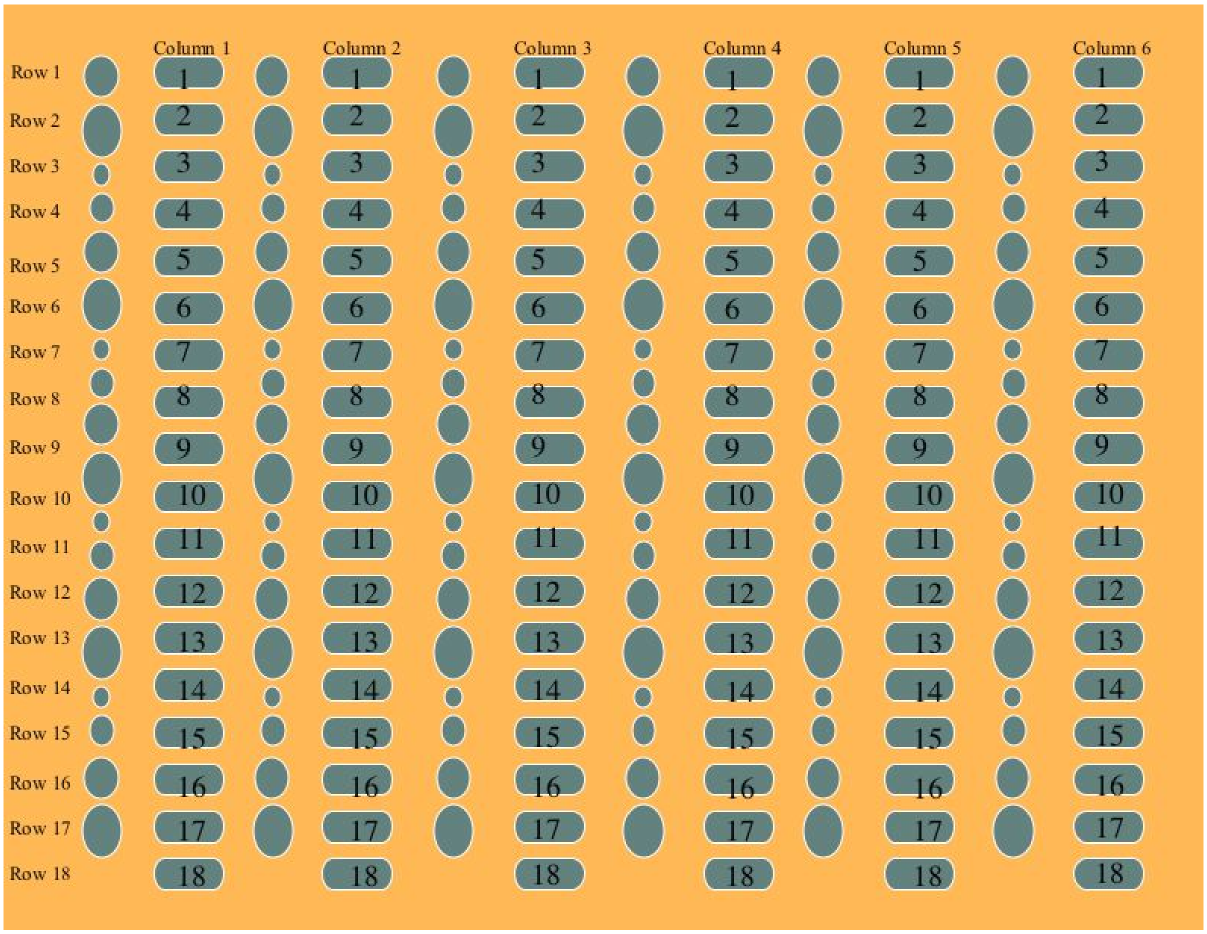

Figure 3.6: Schematic of CSD $BaTiO_3$ Film with Platinum Electrodes

3.6 Statistical Analysis of the Data

Two statistical techniques were used to analyze the data from this experiment. Before any analysis, simple calculations of the mean and standard deviation of capacitance and loss tangent were performed on each data set. Refer to Appendix B for the data compiled in this experiment. Next, the data integrity was checked using JMP to find out what type of distribution the data belonged to. Since the data did not belong to the normal distribution, nonparametric methods were then deployed utilizing JMP to find out if any statistical differences existed among the nine samples.

3.6.1 Mean and Standard Deviation of Loss Tangent and Capacitance

By examining the mean and standard deviation of the loss tangent and capacitance responses, quick assessments can be made about the re-oxidation anneal process, see Table 3.3 and 3.4. The goal is to minimize the loss tangent and maximize capacitance with as little variation as possible. The 550°C/10^{-5} Torr and 550°C/10^{-3} Torr levels yielded a lower loss tangent and smaller standard deviation. The 450°C/10^{-4} Torr or the 450°C/10^{-5} Torr setting yielded a higher capacitance. For the loss tangent response, at 450°C/10^{-5} Torr, 450°C/10^{-4} Torr, 450°C/10^{-3} Torr, and 650°C/10^{-4} Torr, the standard deviation is larger than the other levels. For the loss tangent response, a small change can have a large effect on the quality of the capacitor. Therefore, even though the capacitance is high at 450°C/10^{-4} Torr and 450°C/10^{-5} Torr, these levels may not be acceptable because the loss tangent response is larger. The loss tangent response is more crucial in device reliability than the capacitance, therefore that is the response this thesis focuses on. Hence, by examining Table 3.5, it is important to explore 550°C/10^{-5} Torr and 550°C/10^{-3} Torr levels and the relationship with the loss tangent response. These are preliminary observations that are verified using statistical analysis in subsequent sections of this paper.

Table 3.4: Loss Tangent Mean and Standard Deviation by Temperature and Pressure

Pressure (Torr)	450	550	650
10^{-3}	μ=.05325 s=.01028 N=40	μ=.02805 s=.00332 N=38	μ=.04043 s=.00717 N=40
10^{-4}	μ=.04381 s=.0182 N=37	μ=.03222 s=.008802 N=27	μ=.06168 s=.01636 N=25
10^{-5}	μ=.03831 s=.0101 N=39	μ=.0275 s=.00279 N=40	μ=.03411 s=.00954 N=38

Temperature (^{o}C)

Table 3.5: Capacitance Mean and Standard Deviation by Temperature and Pressure

Pressure(Torr)	450	550	650
10^{-3}	μ=1.2447 s=.22234 N=40	μ=1.24892 s=.08987 N=38	μ=1.2955 s=.04947 N=40
10^{-4}	μ=1.50541 s=.11926 N=37	μ=1.25404 S=.04264 N=27	μ=.97672 s=.06272 N=25
10^{-5}	μ=.1.46823 s=.11381 N=39	μ=1.37263 S=.09944 N=40	μ=.89774 s=.04133 N=38

Temperature (^{o}C)

3.6.2 Checking the Distribution of the Data

Before beginning a design of experiment, one must understand the data as well as the problem. Typically, finding the probability distribution of the data is performed to relate the values of the response characteristic (loss tangent) to their probability of occurrence in a population. Some typical probability distributions for continuous response data (used in this research) are:

- Normal distribution
- Student's *t*-distribution
- Chi-Squared distribution

- F distribution
- Continuous Uniform distribution
- Exponential distribution

The most common distribution is the normal distribution, and this is the distribution most statistical process control techniques (ANOVA, control charts, process capability) are based on for continuous response data. Typically, a normal analysis is performed on the data to find out to what type of statistical distribution the data belongs. A fallacy of analyzing data is assuming normal data and performing hypothesis testing when the distribution of the data does not fit that assumption. Most mean hypothesis tests assume a normal distribution. Normal analysis was performed on the response loss tangent. The hypothesis test performed on the nine samples is:

$$\begin{aligned} H_o &: \ X_i \sim N(\mu,\sigma^2) \\ H_a &: \ X_i \neq N(\mu,\sigma^2) \end{aligned} \tag{3.5}$$

where X_i is the population of each sample ($i=1,\ldots,9$) and N represents the normal distribution with mean, μ, and variance, σ^2. Figures 3.7-3.15 show frequency distributions of the loss tangent response at the nine temperature and pressure combinations. Only one sample exhibited a close to normal distribution, see Figure 3.9. The Shapiro-Wilk's W Statistic is used to determine if the distribution is normal and is represented as a p-value in this paper. If the W statistic is significant (p-value<.05) for a treatment, then the null hypothesis for normality should be rejected [27]. Table 3.6 shows the results from the hypothesis tests for normality; only the 450°C/10^{-3} Torr treatment, see Figure 3.9, was not rejected for normality at the 5% significance level.

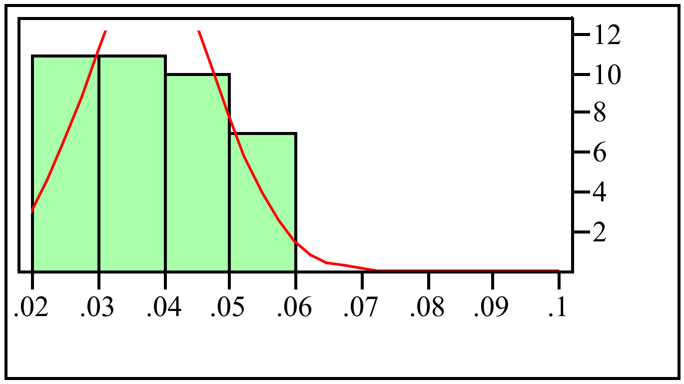

Figure 3.7: Fitted Normal Distribution for Loss Tangent at 450°C/10^{-5} Torr

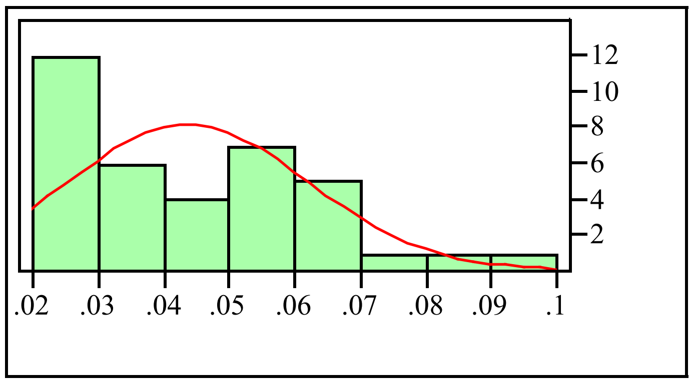

Figure 3.8: Fitted Normal Distribution for Loss Tangent at 450°C/10^{-4} Torr

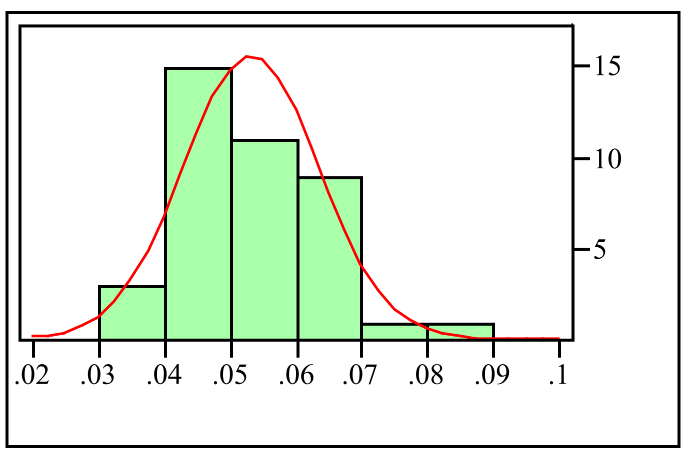

Figure 3.9: Fitted Normal Distribution for Loss Tangent at 450°C/10^{-3} Torr

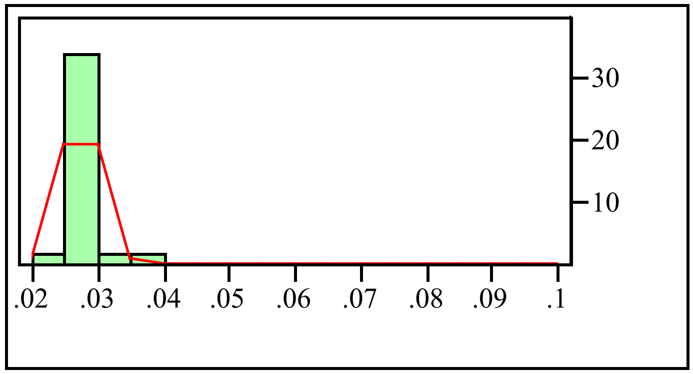

Figure 3.10: Fitted Normal Distribution for Loss Tangent at 550°C/10^{-5} Torr

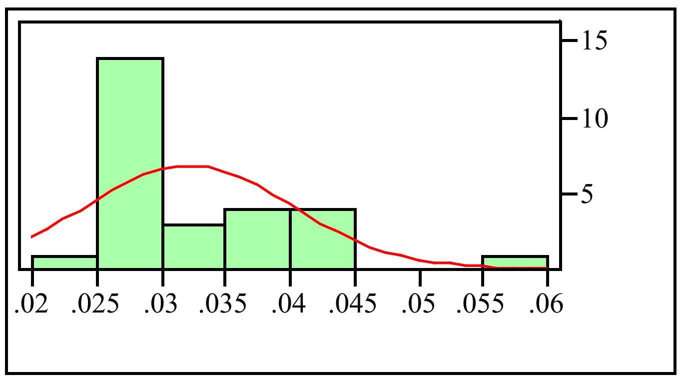

Figure 3.11: Fitted Normal Distribution for Loss Tangent at 550°C/10^{-4} Torr

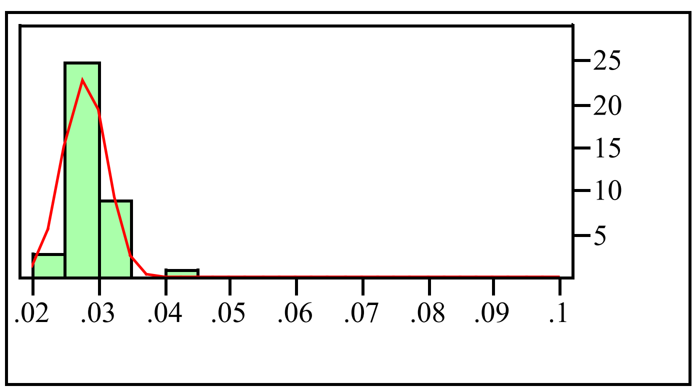

Figure 3.12: Fitted Normal Distribution for Loss Tangent at 550°C/10^{-3} Torr

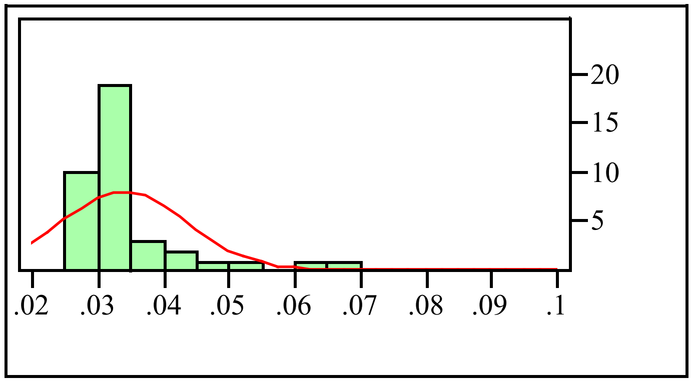

Figure 3.13: Fitted Normal Distribution for Loss Tangent at 650°C/10^{-5} Torr

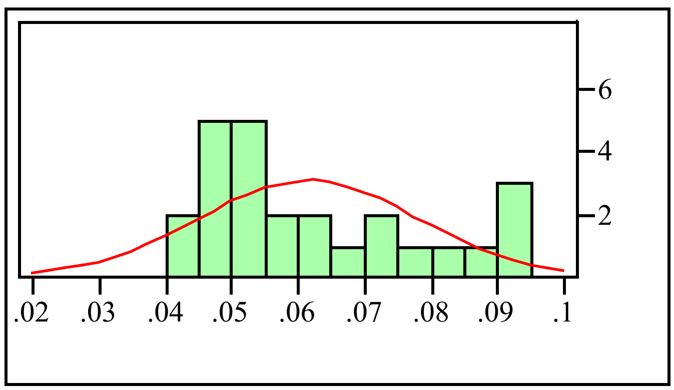

Figure 3.14: Fitted Normal Distribution for Loss Tangent at 650°C/10^{-4} Torr

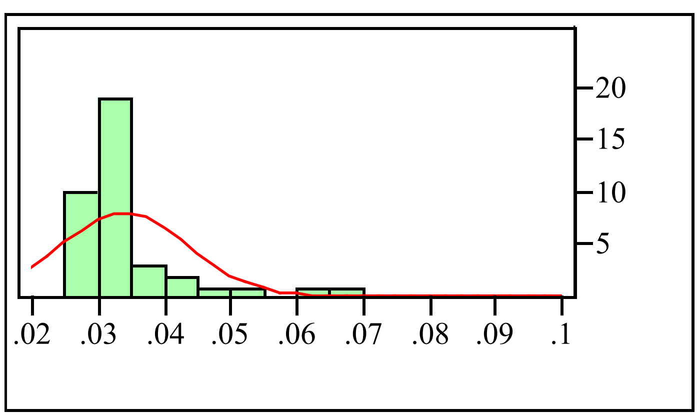

Figure 3.15: Fitted Normal Distribution for Loss Tangent at 650°C/10^{-3} Torr

Table 3.6: W Statistic results from Hypothesis Test for Normality

Temperature	Pressure	N	p-value
450	10^{-5}	39	.0166
450	10^{-4}	37	.0048
450	10^{-3}	40	0.1159
550	10^{-5}	40	<.0001
550	10^{-4}	27	.0002
550	10^{-3}	38	.006
650	10^{-5}	38	<.0001
650	10^{-4}	25	.0226
650	10^{-3}	40	<.0001

Other information can be inferred about the distributions of the data. For example, the 450°C/10^{-4} Torr distribution in Figure 3.8 looks as if there are at least two distributions present by the two different bell-like shapes in the histogram. This could indicate that there is something else that is changing on the film that is affecting the loss tangent response other than the processing conditions. For example, there could not have been enough randomization across the film in choosing which row and column to test capacitors. Another reason is that the histogram widths are too small.

Typically, if the data are not normal, one can mathematically transform the data to infer useful information from it. The data were transformed using the following methods: $\sqrt[4]{y}$, $\sqrt{y}$, y^2, $\frac{1}{y}$, $\log(y)$, $\exp(y)$, $\frac{1}{\log(y)}$, and $\frac{1}{y^2}$. Other distributions were fitted using JMP, including: Weibull, exponential and gamma. None of these distributions would fit the data in this research. Therefore, parametric techniques such as means testing using Analysis of Variance (ANOVA) cannot be used on these data and some nonparametric techniques must be used in order to reduce Type I and Type II errors. Type I errors are defined as rejecting the null hypothesis (H_o) when it is true and Type II errors are not rejecting H_o when it is false [28].

3.6.3 Analyzing the Data Using Nonparametric Tests

Nonparametric methods are used when the mean, standard deviation and even distribution of a response are not known. These are distribution free methods used to compare groups or paired groups of data [29]. For nonparametric data, or when the data are not normal, testing the mean response is not a worthwhile pursuit. Nonparametric methods assume: random sampling, independent samples, and independent observations [30]. However, disadvantages of using nonparametric tests are:

- They are less efficient than parametric tests
- They will require a larger sample size than parametric tests [31]
- They will disregard some information in the data [22]

Nonparametric tests assign ranks to data rather than checking the spacing between the responses as in ANOVA testing, making it a less powerful test.

3.6.3.1 Testing All Population Medians

A median test measures whether individual treatment medians are greater than the overall median. This test can be used if the data does not have a symmetric distribution because the median will not equal the mean. In this research, the median test was used to determine if there were differences in the medians of the nine treatment combinations of temperature and pressure from the overall median, see Figure 3.16. This figure gives a visual of the responses across all treatments. The box plot shows where the 25%, 50% (median) and 75% quartiles are. One can glance quickly at the figure and see where each treatment median is in relation to others. In examining the response of loss tangent at the nine different temperatures and pressures, a median test was performed:

$$H_o: \begin{array}{l} Median_{450/-3} = Median_{450/-4} = Median_{450/-5} = Median_{550/-3} = Median_{550/-4} = \\ Median_{550/-5} = Median_{650/-3} = Median_{650/-4} = Median_{650/-5} \end{array} \tag{3.6}$$

H_a: *Otherwise*

The p-value test statistic can be determined using a chi-squared distribution with number of samples tested-1 degrees of freedom. In Table 3.7, the p-value "is the probability of obtaining by chance alone a Chi-square value larger than the one calculated if, in reality, the distributions across factor levels are centered at the same location. Observed significance probabilities of 0.05 or less are often considered evidence that the distributions across factor levels are not centered at the same location," meaning that the medians are not the same [32]. The p-value results in Table 3.7 show us that the p-value is <.001. Therefore, using the 5% significance level, we can say there is a difference between the medians of the nine populations. However, from Figure 3.16, we can see that the populations at $550/10^{-3}$ and $550/10^{-5}$ both yielded lower loss tangent responses than the other responses. Let's examine those two responses to see if there is a difference between their medians.

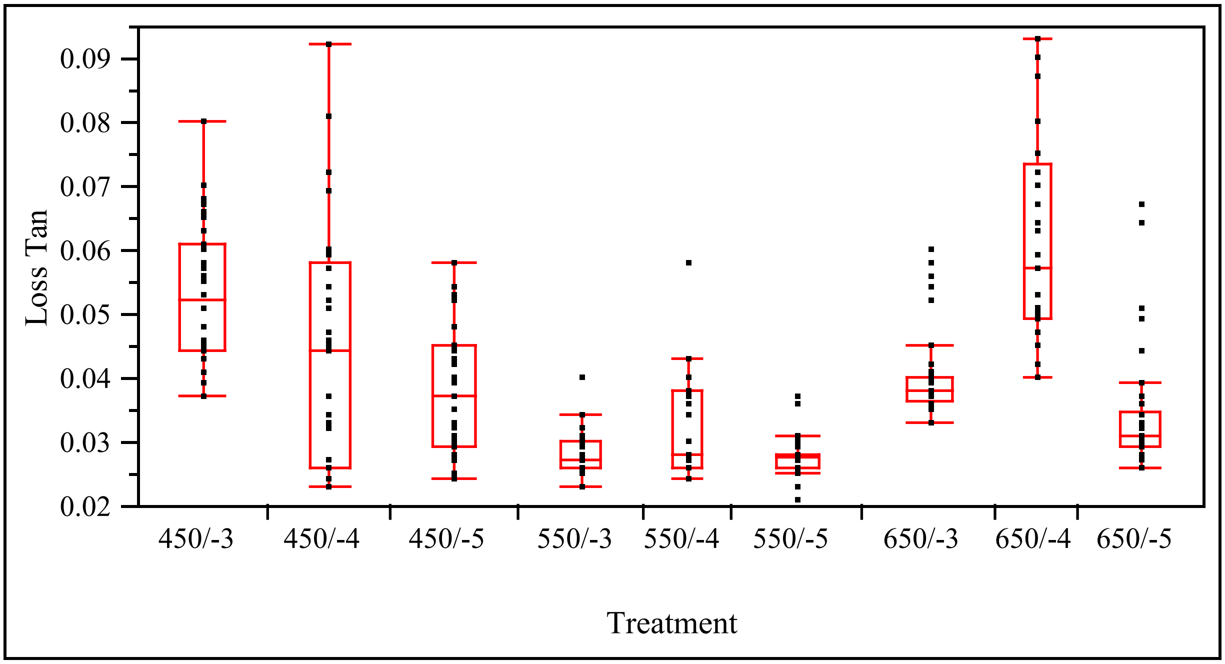

Figure 3.16: Box Plot of Loss Tangent for all 9 Samples

Table 3.7: Chi-Square Approximation for p-value of 9 Samples

Chi-Square	Degrees of Freedom	p-value
165.0271	8	<.0001

3.6.3.2 Testing Two Population Medians

In the previous section, we saw that the responses of $550/10^{-5}$ and $550/10^{-3}$ were much lower than the other seven. By examining Figure 3.17, we can see that the median of the response is slightly lower at 550/-3, but the range of the response is smaller at $550/10^{-5}$. Let's use the medians test to see if there is a difference in the loss tangent response at these two levels:

$$\begin{aligned} &H_o : Median_{550/-3} = Median_{550/-5} \\ &H_a : Otherwise \end{aligned} \tag{3.7}$$

Since the p-value is greater than .05 (using the 5% significance level), we do not reject H_o in Table 3.8. The conclusion can be made there is not a significant difference in the loss tangent medians of 550/10^{-5} and 550/10^{-3}. Therefore, from these data we cannot conclusively say there is a difference of re-oxidation anneal furnace levels at 10^{-5} Torr or 10^{-3} Torr at 550°C.

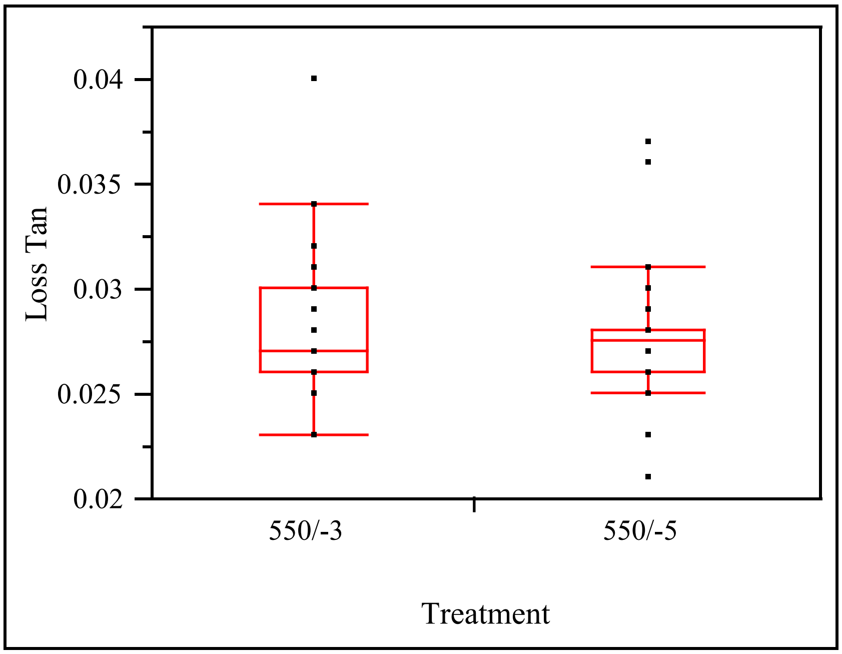

Figure 3.17: Box Plot of Loss Tangent for 550/-3 and 550/-5

Table 3.8: Chi-Square Approximation for p-value of 2 Samples

Chi-Square	Degrees of Freedom	p-value
0.0533	1	0.8174

3.6.4 Conclusions

Based on the nonparametric tests performed, there was a statistically significant difference in the loss tangent response from all nine treatments of 450°C/10^{-5} Torr, 450°C/

10^{-4} Torr, 450°C/10^{-3} Torr, 550°C/10^{-5} Torr, 550°C/10^{-4} Torr, 550°C/10^{-3} Torr, 650°C/10^{-5} Torr, 650°C/10^{-4} Torr, and 650°C/10^{-3} Torr. Two of the treatments, 550°C/10^{-5} Torr and 550°C/ 10^{-3} Torr, yielded lower loss tangent responses. Nonparametric tests were performed on these two responses and there is no statistical difference in the medians of these two responses. 550°C/10^{-5} Torr yielded the lowest loss tangent response with a smaller sample standard deviation, see Table 3.4 in Section 3.6.1. Therefore, 550°C/10^{-5} Torr is used in an additional design of experiment that is run to examine the area around 550°C and 10^{-5} Torr to determine if better levels exist in the local area to operate the re-oxidation anneal furnace.

3.6.4.1 Recommendations and Lessons Learned

This experiment was conducted at the very beginning of this research. There were several opportunities for improvements that can also be corrected during the next experiment. The measurement process can be improved by randomly choosing which capacitors to test rather than testing capacitors in the same column or same area of the film. By testing capacitors from across the film, we screen out location effects and other factors that could be causing variation in our data. In addition, there are also other factors such as the film position during deposition, the crystallization anneal, and position in the oven during the crystallization anneal that must be considered in conjunction with analyzing the effects of temperature and pressure in the re-oxidation anneal furnace.

CHAPTER 4

SECOND EXPERIMENT WITH THE RE-OXIDATION ANNEAL: A 2^2 DESIGN OF EXPERIMENT

In the previous section, we determined that a statistically significant difference exists in the response loss tangent at different temperature and pressure levels. In particular, we observed that at 550°C and 10^{-5} Torr, we obtained a lower mean and smaller standard deviation. We further observed that at 550ºC, there is no statistically significant difference between the response loss tangent at the pressure levels of 10^{-5} and 10^{-3} Torr.

The purpose of this next experiment is to determine if the local area around the temperature at 550ºC and pressure at 10^{-5} Torr can yield a lower loss tangent and to find out how the temperature and pressure in the re-oxidation anneal furnace affects the loss tangent within this local area. We performed another designed experiment using a finer grid to examine the temperature and pressure levels. We used lessons learned from the first experiment. A full factorial, two factor, two level, or 2^2 experiment is conducted with centerpoints, as shown in Table 4.1.

Table 4.1: 2^2 Full Factorial Experiment: Factors and Levels

Factor	Levels	Blocks
Temperature(°C)	500, 550, 600	Crystallization Anneal: 1, 2 Complete Block
Pressure (Torr)	$5x10^{-6}$, 10^{-5}, $2x10^{-5}$	Film Position in Crystallization Anneal: 1,2,3,4 Complete Block within Anneal

4.1 Experimental Design

In this next study, a 2^2 design of experiment with one center point is analyzed. It provides 5 different responses for each Crystallization Anneal block. The factors examined are temperature and pressure. The specific levels for pressure were chosen because $5x10^{-6}$ Torr and $2x10^{-5}$ Torr are both equidistant from 10^{-5} on a log scale, where both are $\log_{10}(2)$ away from 10^{-5} Torr. In addition, two different blocks were added: Crystallization anneal order and film position in the crystallization anneal furnace. A block is used when an undesired influence or nuisance factor affects the variability [23]. Films from two different crystallization anneals are analyzed to find out if there is film to film variation. Film position in the furnace during the crystallization anneal is considered as a block since a strip of four films (uncut) and an additional film that is used for the center point are annealed together in the crystallization furnace. Film position is studied nested within Crystallization Anneal order to determine if there are differences from each anneal.

Therefore, the experiment is run as two experiments, where film position in the furnace is randomized as a complete block within Crystallization Anneal Order. However, anneal is confounded with film position. See Tables 4.2 and 4.3 for an experimental layout. The procedures in 3.5.1 were repeated for this experiment. The only major change is the use of randomization in selecting which capacitors to measure on each film.

Table 4.2: Crystallization Anneal 1 Block

		Pressure (Torr)	
		5x10-6	**2x10-5**
Temperature (°C)	**500**	Film Position 2	Film Position 4
	600	Film Position 3	Film Position 1

Table 4.3: Crystallization Anneal 2 Block

		Pressure (Torr)	
		5x10-6	**2x10-5**
Temperature (°C)	**500**	Film Position 4	Film Position 1
	600	Film Position 2	Film Position 3

4.2 Statistical Analysis

4.2.1 Mean and Standard Deviation of Loss Tangent

For this experiment, the mean, standard deviation and numbers of samples for each Crystallization Anneal were calculated. These results are shown in Tables 4.4 and 4.5. As with the other experiment, at 550°C and 10^{-5} Torr, the loss tangent response for both anneals yielded a lower loss tangent response. Therefore, we proceed in our analysis to find out how the data integrity compares to the 3^2 experiment.

Table 4.4: Loss Tangent Mean and Standard Deviation by Temperature and Pressure for Crystallization Anneal 1

Pressure (Torr)	500	550	600
$2x10^{-5}$	μ=0.10687 s=0.02632 N=37		μ=0.08268 s=0.014913 N=36
10^{-5}		μ=0.04983 s=0.00638 N=40	
$5x10^{-6}$	μ=0.11161 s=0.02138 N=34		μ=0.10061 s=0.01883 N=39

Temperature (^oC)

Table 4.5: Loss Tangent Mean and Standard Deviation by Temperature and Pressure for Crystallization Anneal 2

Pressure (Torr)	500	550	600
$2x10^{-5}$	μ=0.12068 s=0.02601 N=39		μ=0.10833 s=0.01542 N=40
10^{-5}		μ=0.04454 s=0.00982 N=39	
$5x10^{-6}$	μ=0.1494 s=0.02058 N=40		μ=0.11205 s=0.0234 N=39

Temperature (^{o}C)

4.2.2 Checking the Distribution of the Data

In this experiment, a histogram and normal distribution fit were performed on all the samples. Appendix C shows these fits. The results from the normal analysis are shown in Table 4.6. Using a 5% significance level in Crystallization Anneal 1, at 600°C and 2x10^{-5} Torr and at 600°C and 5x10^{-6} Torr, the samples were not normal. However, there was a bad O-ring in the re-oxidation furnace during the experiment that may have contributed to the non-normal distribution. From the second anneal, the 600/5x10^{-6} and the 500/5x10^{-6} samples were not normal. However, the 500/5x10^{-6} sample was only marginally not normal. In both anneals, the 600/5x10^{-6} samples were not normal. One reason for this is the lower pressures in the 10^{-6} regime are hard to achieve. However, in both anneals, the center point settings at 550/10^{-5} were normal. Therefore, this is good starting point in analyzing what is happening around these levels. Although the distribution of the response from some treatments are statistically significant from a normal distribution, the histograms are close a normal distribution curve, see Appendix C. Next, we need to find out if the group means are different.

Table 4.6: W Statistics results from Hypothesis Test for Normality for Anneal 1 and 2

Temperature	Pressure	N	Anneal	p-value
600	2x10-5	36	1	0.0205
500	5x10-6	34	1	0.5189
600	5x10-6	39	1	0.0367
500	2x10-5	37	1	0.0591
550	10^{-5}	40	Center point	0.4359
500	2x10-5	39	2	0.2677
600	5x10-6	39	2	0.0087
600	2x10-5	40	2	0.1373
500	5x10-6	40	2	0.0416
550	10^{-5}	39	Center point	0.2072

4.2.3 Single Factor ANOVA

Analysis of Variance (ANOVA) is referred to by DeVor as "a collection of experimental situations and statistical procedures for the analysis of quantitative responses from experimental units." Data that are normally distributed can be used in ANOVA to determine the effects of one or more factors [28]. A *t* test can be used to test the means of two groups, or if one has more than two groups, an *F* test can be used. An *F* test is a ratio of the sum of squares. This ratio is then compared to the *F* Distribution table and a p-value is calculated [23]. This information is then put into an Analysis of Variance table.

An ANOVA was performed to compare the five different treatments of temperature and pressure combinations. Figures 4.1 and 4.2 show the box plots from each of the two anneals. Using the 5% significance level, Tables 4.7 and 4.8 show the p-value is <0.0001 for both Crystallization Anneal 1 and 2. Therefore, the five treatments are statistically different. Since the goal is to decrease the loss tangent response, the recommendation is made to use the treatment 550/-5, since it yielded a lower response and had less variation than the other four treatments in both Anneal 1 and 2.

Although it appears running the re-oxidation furnace at 550°C and 10^{-5} Torr yields a lower loss tangent, we do not know for certain until we do more analysis. We also want to know how each factor, temperature and pressure, affects the response, loss tangent. However, to do that, we must use a tool that shows us how multiple factors can change the response.

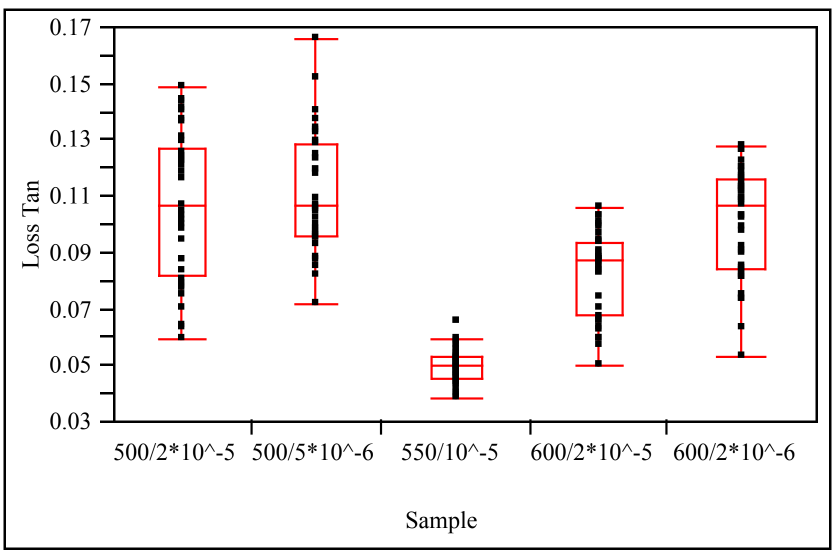

Figure 4.1: Box Pot for Anneal 1

Table 4.7: Analysis of Variance Anneal 1

Source	DF	Sum of Squares	Mean Square	F Ratio	Prob > F
Sample	4	0.09721962	0.024305	69.9813	<.0001
Error	181	0.06286238	0.000347		
C. Total	185	0.16008200			

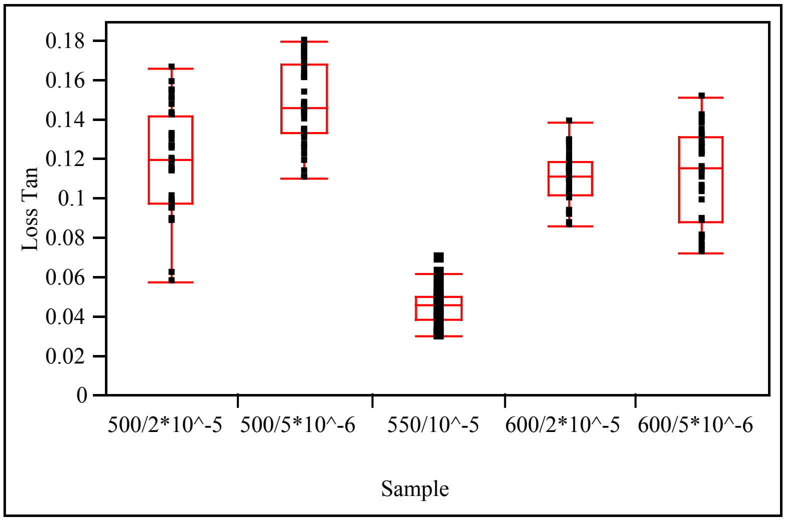

Figure 4.2: Box Pot for Anneal 2

Table 4.8: Analysis of Variance Anneal 2

Source	**DF**	**Sum of Squares**	**Mean Square**	**F Ratio**	**Prob > F**
Sample	4	0.23240372	0.058101	144.7858	<.0001
Error	192	0.07704746	0.000401		
C. Total	196	0.30945118			

4.2.4 Response Surface Analysis

Response Surface Analysis allows us to model a response that is affected by one or more variables. A response surface is a tool that can be used to analyze a local region of an experiment to determine how small changes in temperature and pressure affect the loss tangent. We can determine optimum operating conditions or find a region where operating conditions are satisfied.

The Response Surface Analysis that we use here is a mathematical model that predicts loss tangent as a function of two continuous factors (temperature and pressure). We employed the following model:

$$y = \beta_0 + \beta_1 x_1 + \beta_2 x_2 + \beta_{11} x_1^{\ 2} + \beta_{12} x_1 x_2 + \varepsilon \tag{4.1}$$

where β_o, β_1, β_2, *and* β_{12} are the coefficients, x_1 and x_2 are the factors, temperature and pressure, respectively, and ε is the error. The second order response of the LogPressure, x_2^2, was not included in the model; this was proven in preliminary analysis, not included in this thesis and was excluded in the statistical results. Higher order models can also be used, but with only three levels for each variable, nothing beyond second order interactions can be estimated. It is unlikely a polynomial can accurately model an entire process, but for a small region, it may model the loss tangent response accurately. These designs can be shown graphically as a three dimensional surface, see Figures 4.5 and 4.6, or they can be represented two dimensionally on a contour plot, see Figures 4.11 and 4.12.

Initially, a multi-regression model was performed. Tables 4.11 and 4.12 show the p-values for the effects in each anneal. In this analysis, a 5% significance level was used for all the analysis using least squares or the *F* ratio. Both the main effects of temperature and pressure and their interaction were significant. The quadratic effect of temperature was significant. The quadratic effect of pressure was not significant and was not included in this analysis. Because the experiment was performed in two blocks for crystallization anneal runs, a separate statistical analysis was performed for each.

4.2.4.1 Results of the Analysis

Crystallization Anneal 1 and 2 each contain five samples that were all annealed together at the same time. After the crystallization anneal, each sample was annealed a second time (re-oxidation) at different temperatures and pressures.

The model for this Crystallization Anneal 1 is:

Loss Tangent = 0.02733 – 0.00013Temperature – 0.01907LogPress + 0.00002(Temperature-551.08)*(Temperature – 551.08) -.00022*5* (Temperature-551.08)* (4.2)

The model for this Crystallization Anneal 2 is:

*Loss Tangent =0.04652 –0.00025*Temperature – .02694*LogPress+.00003*(Temperature-550)*(Temperature-550) + 0.00042*5*(Temperature-550)* (4.3)

The R^2 value is the proportion of variation accounted for by the model [22]. The R^2 adjusted value is independent of the number of parameters used in the model. Table 4.9 shows the R^2 adjusted value for the Anneal 1 model as 0.59**,** only a marginally good fitting model. The Anneal 2 had a better R^2 adjusted value of 0.74, see Table 4.10. Typically, R^2 adjusted values greater than .80 are desired. However, these values are high enough to model the response in this experiment.

Table 4.9: Summary of Fit Crystallization Anneal 1

R^2	0.607311
R^2 Adj	0.598633
Root Mean Square Error	0.018636
Mean of Response	0.089476
Observations (or Sum Wgts)	186

Table 4.10: Summary of Fit Crystallization Anneal 2

R^2	0.751019
R^2 Adj	0.745832
Root Mean Square Error	0.020032
Mean of Response	0.107221
Observations (or Sum Wgts)	197

In Tables 4.11 and 4.12, the ANOVA table displays a F-ratio of 69 for Anneal 1 and an F-ratio of 144 for Anneal 2. An effect with a F-ratio of greater than 2 is considered important to keep in the model. Therefore, we can conclude both these models are statistically significant.

Table 4.11: Analysis of Variance Crystallization Anneal 1

Source	DF	Sum of Squares	Mean Square	F Ratio
Model	4	0.09721962	0.024305	69.9813
Error	181	0.06286238	0.000347	Prob > F
C. Total	185	0.16008200		<.0001

Table 4.12: Analysis of Variance Crystallization Anneal 2

Source	DF	Sum of Squares	Mean Square	F Ratio
Model	4	0.23240372	0.058101	144.7858
Error	192	0.07704746	0.000401	Prob > F
C. Total	196	0.30945118		<.0001

In Tables 4.13 and 4.14, the *Effects Tests* gives *F* ratios and p-values for each effect included in the model. Since the *F ratios* for each of the effects (Temperature, LogPress, Temperature*Temperature, LogPress*Temperature) are all greater than 2 and the p-values are all less than 0.05, these effects are all significant in both Anneal 1 and 2 models. Therefore, the Temperature, LogPress, Temperature*Temperature, and LogPress*Temperature effects are significant at a 5% significance level for both models. In Anneal 1, the LogPress*Temperature effect is only marginally significant with a p-value of 0.03, but it is still less than 0.05.

Table 4.13: Effect Tests Crystallization Anneal 1

Source	Nparm	DF	Sum of Squares	F Ratio	Prob > F
Temperature&RS	1	1	0.00634920	18.2813	<.0001
LogPress&RS	1	1	0.00480117	13.8240	0.0003
Temperature*Temperature	1	1	0.08037957	231.4374	<.0001
LogPress*Temperature	1	1	0.00158257	4.5567	0.0341

Table 4.14: Effect Tests Crystallization Anneal 2

Source	Nparm	DF	Sum of Squares	F Ratio	Prob > F
Temperature&RS	1	1	0.02438899	60.7766	<.0001
LogPress&RS	1	1	0.01038983	25.8912	<.0001
Temperature*Temperature	1	1	0.19064921	475.0922	<.0001
Temperature*LogPress	1	1	0.00617430	15.3862	0.0001

In Tables 4.15 and 4.16, the *Parameter Estimates* are another method of finding out which effects are significant. For a one degree of freedom effect, the *t Ratio* is the $\sqrt{F\ Ratio}$ in Tables 4.13 and 4.14. The *Parameter Estimates* uses a hypothesis test to test if the coefficients (intercept, Temperature, LogPress, Temperature*Temperature, LogPress*Temperature) are equal to zero. Therefore, the *t* test rejects that the coefficients are 0 in both models.

Table 4.15: Parameter Estimates Crystallization Anneal 1

Term	Estimate	Std Error	t Ratio	Prob>|t|
Intercept	0.0273325	0.030477	0.90	0.3710
Temperature&RS	-0.000132	0.000031	-4.28	<.0001
LogPress&RS	-0.019066	0.005128	-3.72	0.0003
(Temperature-551.075)*(Temperature-551.075)	0.0000202	0.000001	15.21	<.0001
(LogPress+5)*(Temperature-551.075)	-0.000219	0.000103	-2.13	0.0341

Table 4.16: Parameter Estimates Crystallization Anneal 2

Term	Estimate	Std Error	t Ratio	Prob>|t|
Intercept	0.0465172	0.032097	1.45	0.1489
Temperature&RS	-0.000249	0.000032	-7.80	<.0001
LogPress&RS	-0.02694	0.005295	-5.09	<.0001
(Temperature-550)*(Temperature-550)	0.0000312	0.000001	21.80	<.0001
(Temperature-550)*(LogPress+5)	0.0004154	0.000106	3.92	0.0001

Checking the normality of the residuals of the model is often more helpful in determining how reliable the model is that we use. Figures 4.3 and 4.4 show the normal quantile plot for each anneal. According to Montgomery, more emphasis should be placed on the middle of the straight line plot versus the extreme values. Also, moderate departures from normality should not be of great concern [23]. If a residual is substantially larger than the others, then that point should be investigated to find out what happened in the process. This can distort the analysis of variance. However, this outlier should not be discarded unless the reason for the difference has been determined. Usually, if the distribution is highly non-normal, then there are other phenomena occurring in the data that have not been taken into consideration with this model [22]. The p-value or W Statistic is greater than 0.05 for both Anneals. Therefore, there is not significant evidence that suggests residuals for the model are not normal at the 5% significance level. Therefore, we can be reasonably confident these models accurately reflect how the temperature and pressure in the re-oxidation anneal affects loss tangent and have no reason to question the models.

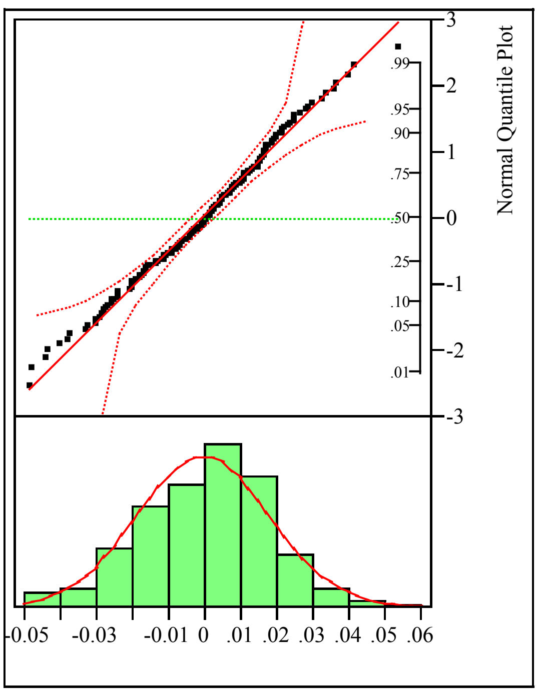

Mean	-5.05e-16
Std Dev	0.0184336
N	186
p-value	0.6193

Figure 4.3: Normal Analysis of Residuals: Crystallization Anneal 1

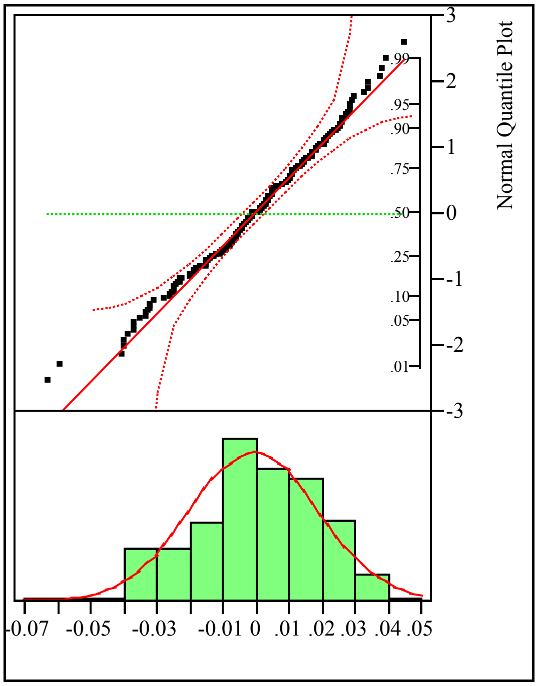

Mean	-3.98e-16
Std Dev	0.0194694
N	195
p-value	0.1668

Figure 4.4: Normal Analysis of Residuals: Crystallization Anneal 2

4.2.4.2 Differences Between Anneal 1 and Anneal 2

The response surface for each anneal is shown in Figures 4.5 and 4.6. These depict loss tangent as a function of temperature pressure. The x and y axes ranges are the same in both models. These surfaces show a distinct valley for each of the annealing models. Visually, we can see that the local minimum for loss tangent occurs at a temperature of 550 and LogPress at -4.7 for both annealing models. The models in Figure 4.7 and 4.8 show loss tangent sloping downward as the pressure increases. The negative slope is very critical because this disproves our theory that 550°C and 10^{-5} Torr are the levels that yield the lowest loss tangent. Our model implies 550/-4.7 is the best setting to yield the smallest loss tangent. But we cannot conclusively say –4.7 or $2x10^{-5}$ Torr yields a lower loss tangent.

From the first DOE, we did conduct this experiment at 550°C and 10^{-4} Torr. However, these data did not yield a lower loss tangent and had much more variation than

550/ 10^{-3} and 550/10^{-5} levels. But, we do not conclusively know what caused this larger response and variation. Therefore, we cannot rely on these data. In order to discern if running the re-oxidation furnace at higher pressures would yield a lower loss tangent, we would need to run more experiments in the local region around 550°C and $10^{-4.7}$ Torr. We would only examine the local region because the response surface models work better for smaller areas, and response surface analysis is a sequential process since it only works in small regions.

Now, how are these models different? The response surfaces look similar and have similar curvatures. Both surfaces have curvature in the temperature direction, but not the LogPress direction. This lack of curvature is a result of excluding the LogPress*LogPress effect because it was not significant in the model. The slopes of the models in the LogPress direction are approximately the same. This model can also be used to find the stationary point of the model. This critical point can be a minimum or maximum; however, this critical point was not considered in this research because it was outside of the feasible ranges for temperature and pressure.

The two Crystallization Anneal models are distinctly different in the curvatures due to the Temperature*Temperature effect. This can be seen in Figures 4.9 and 4.10. Anneal 2 shows more sensitivity to the temperature and responds more quickly to changes. Anneal 1 has less curvature and responds less quickly to changes in temperature due to the Temperature*Temperature effect in the model. We can also see in the contour plot in Figures 4.11 and 4.12, different responses due to the different curvatures. Anneal 2 shows several different contours, where Anneal 1 only shows two because the loss tangent is not changing as much as in Anneal 2 within the same ranges for Temperature and LogPress.

Therefore, we can say there is a difference between the two anneals. The sensitivity to the temperature changes is consistent with the equation 3.2 introduced in section 3.2 for the oxygen vacancy concentration, $\left[V_o^{\bullet\bullet}\right]$.

$$\left[V_o^{\bullet\bullet}\right]=\left[\frac{1}{4}pO_2^{-\frac{1}{2}}\exp(\frac{-\Delta H}{RT})\right]^{\frac{1}{3}}[13,25] \qquad (3.2)$$

The oxygen vacancy concentration in a dielectric corresponds to the electrical reliability of the film. In this equation, the oxygen vacancy concentration is directly proportional to the partial pressure of oxygen, pO_2. While the oxygen vacancy concentration is exponentially proportional to the temperature, T, so changes in temperature affect the oxygen vacancy concentration more dramatically than pO_2. The oxygen vacancy concentration is directly related to the insulation resistance (IR). Films with a poor insulation resistance have a higher loss tangent [13]. Therefore, oxygen vacancy concentration may be related to the loss tangent.

What changed between those two anneals? Were the two crystallization anneals different? Were the re-oxidation anneals different? Experimentally, we know that the operator changed out a bad O-ring after the first anneal. However, we also had a blocking effect within each crystallization anneal— the film position in the furnace. For each of the same re-oxidation anneal treatments of temperature and pressure, the film position changed. Therefore, the film position blocking effect is confounded with the anneal block, and its effects cannot be discerned from this experiment. There is no way to determine what caused this effect with these data. To find out, we would have to repeat the experiment on two different anneals, using the same film position in each anneal.

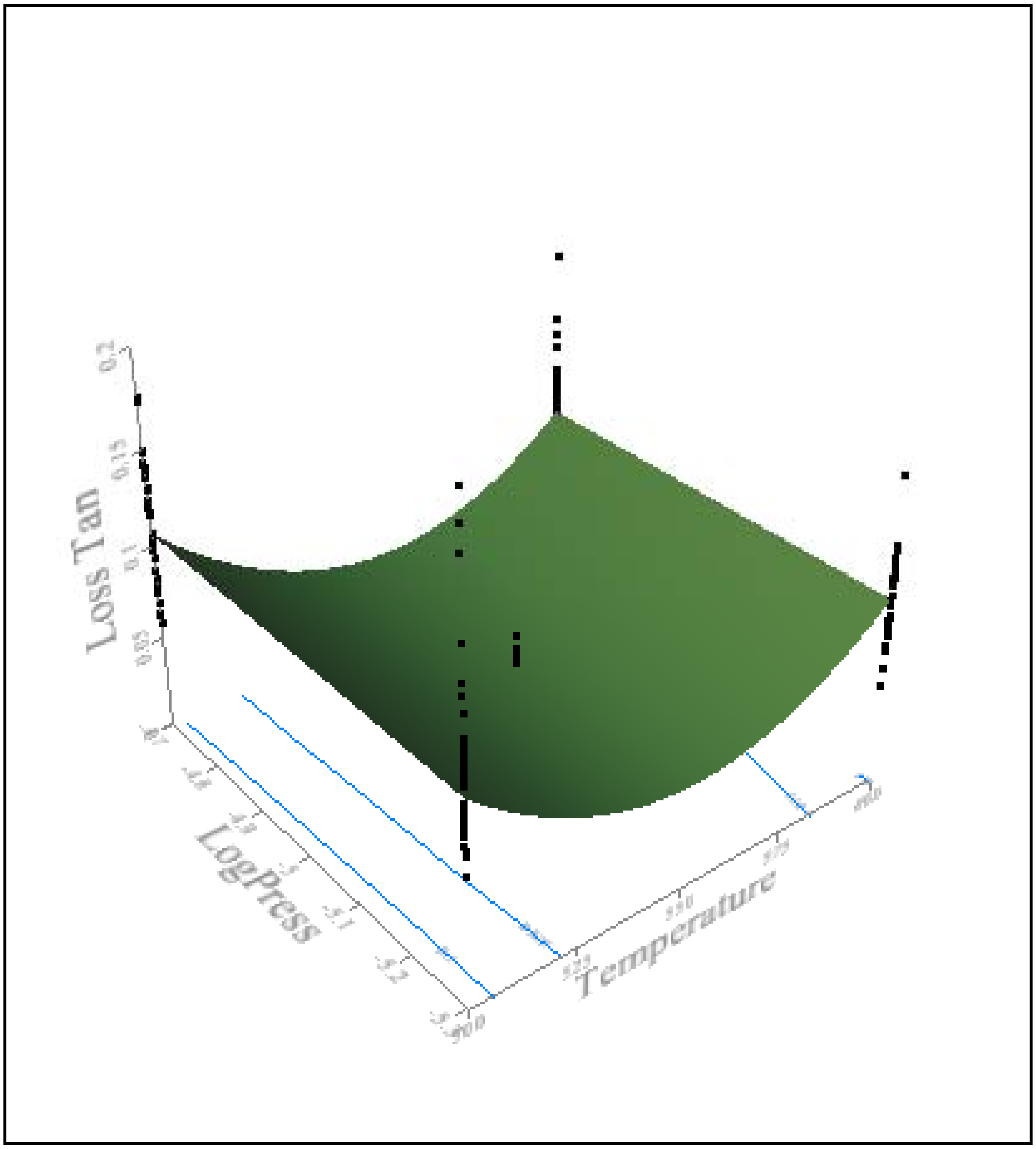

Figure 4.5: Response Surface of Loss Tangent for Crystallization Anneal 1

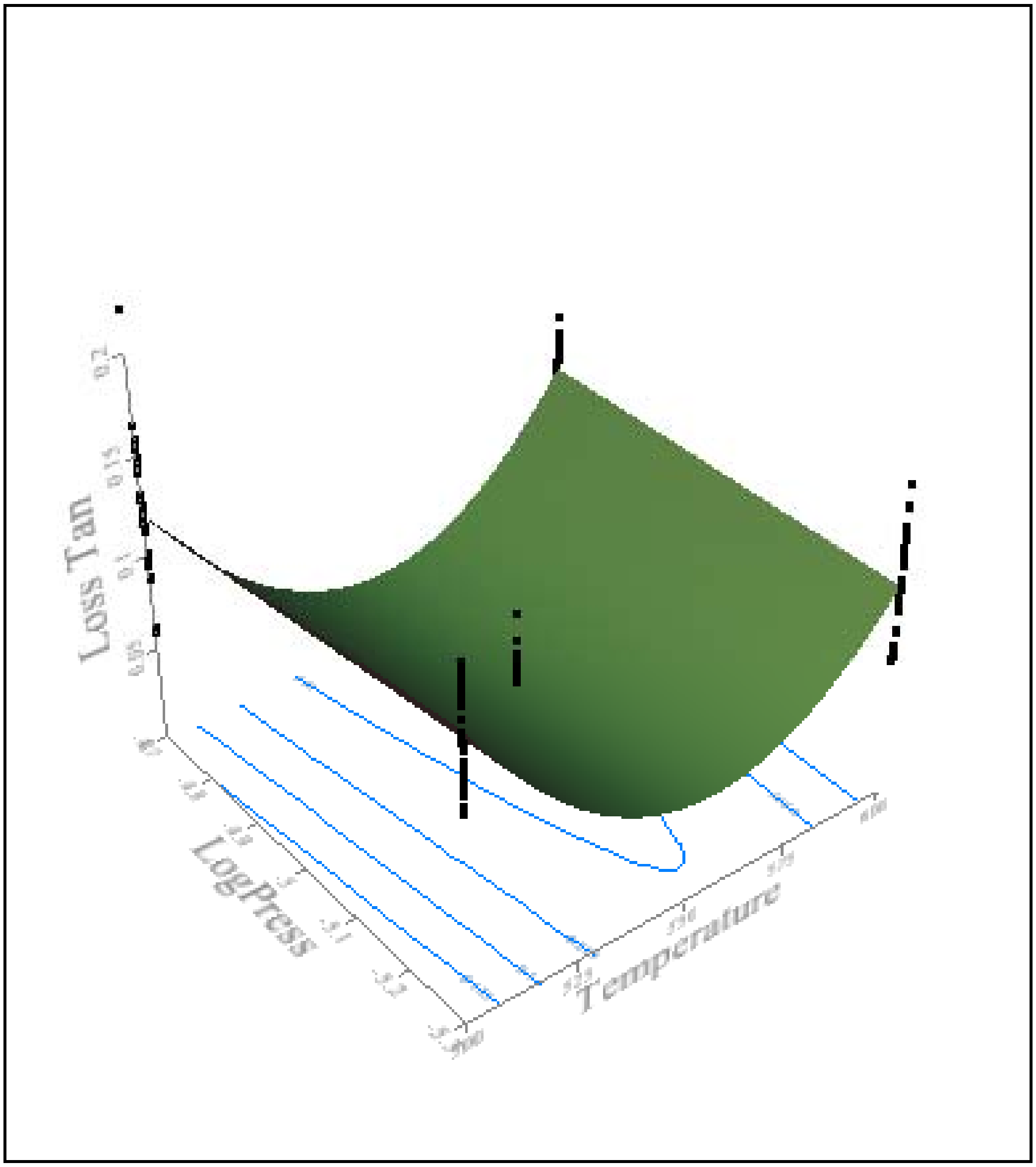

Figure 4.6: Response Surface of Loss Tangent for Crystallization Anneal 2

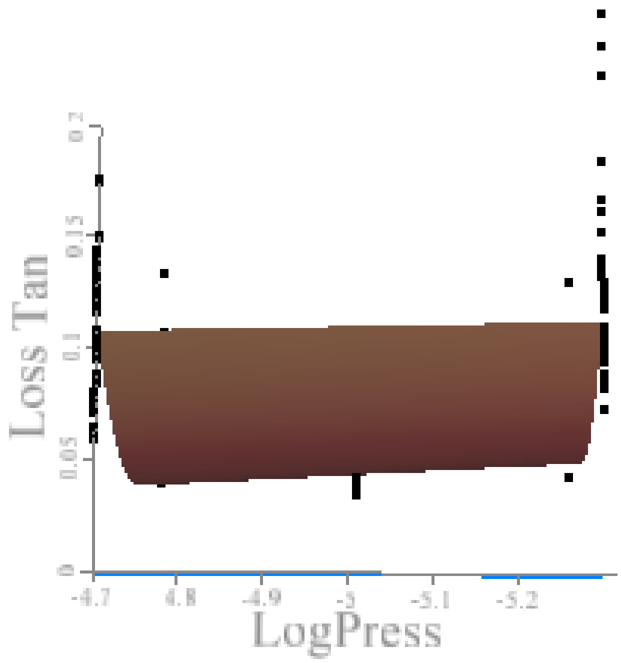

Figure 4.7: Crystallization Anneal 1: Loss Tan vs. LogPress

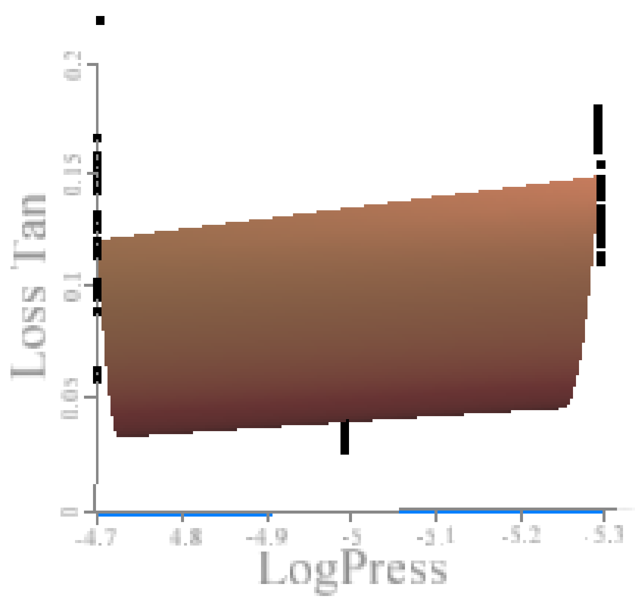

Figure 4.8: Crystallization Anneal 2: Loss Tan vs. LogPress

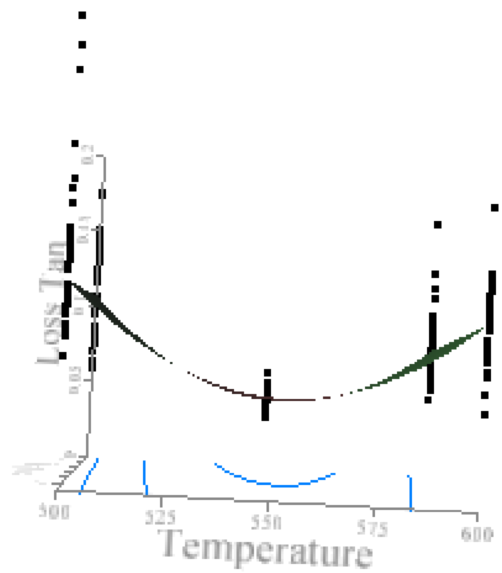

Figure 4.9: Crystallization Anneal 1: Loss Tan vs Temperature

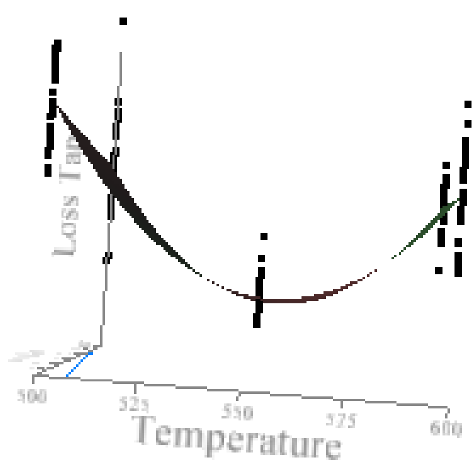

Figure 4.10: Crystallization Anneal 2: Loss Tan vs Temperature

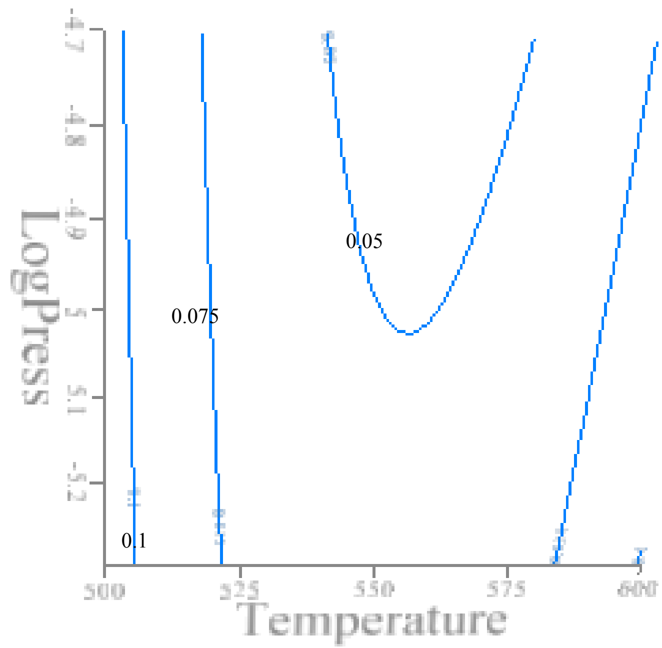

Figure 4.11: Contour Plot of Crystallization Anneal 1: LogPress vs. Temperature

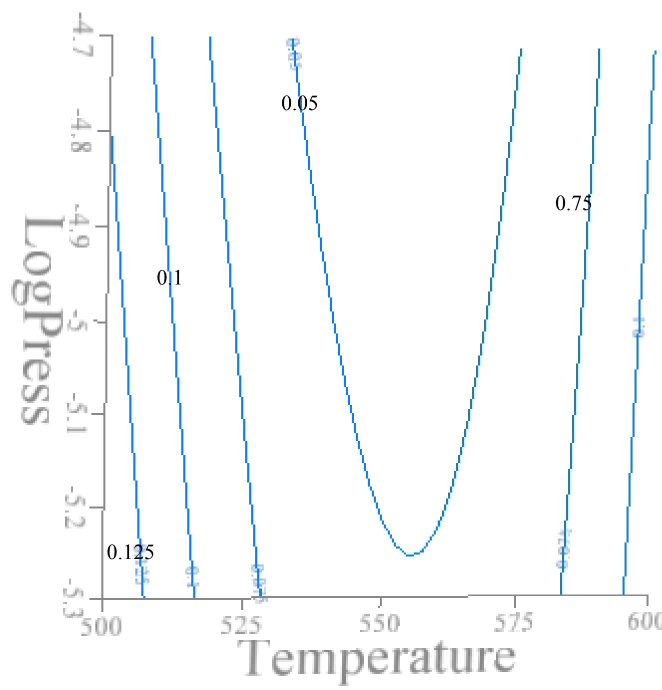

Figure 4.12: Contour Plot of Crystallization Anneal 2: LogPress vs. Temperature

4.2.4.3 Analysis of Combined Crystallization Anneal Models

Another way to examine the effects of the two different crystallization anneals is to combine the two anneals into one model and do an Effects Test to determine if the Crystallization Anneal factor is significant. Initially, we examined the following factors: Temperature, LogPress, Crystallization Anneal, Temperature* Temperature, LogPress*LogPress, Temperature*LogPress, and Crystallization Anneal*Temperature* Temperature. However, LogPress*Temperature, LogPress*LogPress, and Crystallization Anneal were not included in the model because they were proven not to be statistically significant effects. A second order model was fitted with an R^2 adjusted value of 0.69, see Table 4.17. Tables 4.19 and 4.20 show the results from the Effects tests and parameter estimates. The effects test in Table 4.19 show that the *F Ratio* for Crystallization Anneal, Temperature*Temperature was over 2; therefore the interaction between the temperature quadratic term and the Crystallization Anneal is statistically significant. This means that changing one of these factors changes the response. This statistical analysis verifies that the difference we saw in the curvature in the temperature direction of the response surface shown in Figures 4.5 and 4.6 is significant.

Table 4.17: Summary of Fit for Both Crystallization Anneals

RSquare	0.701042
RSquare Adj	0.697878
Root Mean Square Error	0.019879
Mean of Response	0.098603
Observations (or Sum Wgts)	383

Table 4.18: Analysis of Variance for Both Crystallization Anneals

Source	DF	Sum of Squares	Mean Square	F Ratio
Model	4	0.35028161	0.087570	221.5978
Error	378	0.14937697	0.000395	Prob > F
C. Total	382	0.49965858		<.0001

Table 4.19: Parameter Estimates for Both Crystallization Anneals

Term	Estimate	Std Error	t Ratio	Prob>|t|
Intercept	0.0335662	0.022745	1.48	0.1408
Temperature&RS	-0.000187	0.000023	-8.21	<.0001
LogPress&RS	-0.023332	0.003788	-6.16	<.0001
(Temperature-550.522)*(Temperature-550.522)	0.0000258	0.000001	25.66	<.0001
(Temperature-550.522)*(Temperature-550.522)*Crys Anneal Order [1]	-0.000004	4.6e-7	-9.70	<.0001

Table 4.20: Effect Tests for Both Crystallization Anneals

Source	Nparm	DF	Sum of Squares	F Ratio	Prob > F
Temperature&RS	1	1	0.02660514	67.3246	<.0001
LogPress&RS	1	1	0.01499428	37.9432	<.0001
Temperature*Temperature	1	1	0.26026145	658.5944	<.0001
Temperature*Temperature*Crys Anneal Order	1	1	0.03716006	94.0339	<.0001

4.2.4.4 Location Effects

Other effects not considered in this model were rows and columns on the film and film position. We cannot study film position because it is confounded with Crystallization Anneal, but we can study the effects of capacitor position. This is accomplished by looking at the effects of rows and columns. By looking at each of the 10 samples individually to detect if there are any location effects, we can determine if there are any location effects. For example, the $600/10^{-4.7}$ treatment in Anneal 1, columns were determined to not be statistically significant while rows were statistically significant. Therefore, we can conclude there is a statistically significant difference in the means of the rows, but there is no statistically significant difference in the columns. If other samples show this same trend, it may be worthwhile to find out what in the process is causing this location effect across the length of the film, but is having no effect across the width of the film. However, through further analysis, the other four films in Anneal 1 did not show that same trend. Therefore, there may be location effects in this data, but they cannot be discerned in this analysis.

CHAPTER 5

CONCLUSIONS AND RECOMMENDATIONS FOR FUTURE RESEARCH

Our experimental and statistical analysis of the re-oxidation anneal processing conditions resulted in two major findings. The first significant finding of this study was the reliability of the measurement system. The second and more significant finding was that the optimum level for temperature and pressure in the re-oxidation anneal furnace is 550°C and $10^{-4.7}$ Torr.

A Gauge Repeatability and Reproducibility study was conducted to find out what level of confidence we had in our measurement system. The variation in the measurement system, which consisted of the equipment and operator variability should not exceed 10% in order to have confidence in the measurement system. It was found that the variation was 9.23%.

Therefore, we can conclude that the electrical characterization methods used later in this research did produce valid and reliable data.

Next, designed experiments were used to understand more about how temperature and pressure in the re-oxidation furnace affects loss tangent. In the first DOE, while the data were not very useful, valuable lessons were learned. The first is that the seven DOE steps listed in Section 2.5.1 cannot be eliminated or skipped for convenience or to reduce the amount of resources invested in the experiment. There was one major flaw that was not discovered until after the experiment was complete. In the design and experimental phase, randomization and experimental uniformity were not carried out to prevent other sources from variation from affecting the responses. Despite these errors, we did establish a local area to study more in depth. This was accomplished by finding which temperature and pressure levels yielded a lower loss tangent simply by calculating the mean and standard deviation.

The next 2^2 full factorial with a center point corrected these problems and also studied the local area near the 550°C/10^{-5} Torr setting to determine if a better temperature and pressure setting existed. Data from two crystallization anneals were used in a second order response surface design to model the effects of temperature and pressure. Both models were consistent in:

- Identifying temperature, pressure, the interaction between temperature and pressure, and the quadratic term of temperature all as statistically significant factors that affect loss tangent
- Generating approximately the same loss tangent response at each setting and the slopes of the surfaces were the same in the pressure direction.

However, the models were distinctly different in the curvature in the temperature quadratic. Anneal 2 was much more responsive to small changes in temperature, where Anneal 1 was less sensitive to changes in temperature. We do not know if the differences are due to experimental factors introduced by the operator or the equipment or if this difference was due to the different film positions used for different temperature and pressure levels. These two effects are confounded together. My recommendation is to run more experiments from two different anneals, but on the same film positions to find out if there is repeatability from one crystallization anneal to another.

These models did reveal that the re-oxidation furnace temperature level of 550°C yielded a lower loss tangent. In both models, the 10^{-5} Torr was not the optimal setting to lower loss tangent. Increasing the pressure did lower the loss tangent. In this experiment, the pressure level at $10^{-4.7}$ Torr yielded the lowest loss tangent response. Therefore, from this data, we recommend to run the furnace at 550°C and $2x10^{-5}$ Torr. However, since we could decrease the loss tangent by increasing the pressure, the recommendation is made to repeat the experiment by investigating pressures around $2x10^{-5}$ Torr since the response surface analysis is a sequential process and has to be repeated to find the optimal levels. Finally, there are other intrinsic materials properties that may influence the electrical performance of the dielectric that were not studied in this paper. Some controllable properties are: porosity in the film, grain size, metallic migrations, second phases, contaminants, stoichemetry, and deposition procedures [19]. There are also some uncontrollable factors such as microstructure, porosity, humidity, and others that also affect the electrical reliability of the films that should be minimized in order reduce the amount of variation in these measurements.

The loss tangent may be related to the oxygen vacancy concentration. The oxygen vacancy concentration is related to the insulation resistance (IR) of the film. A high insulation resistance indicates a good electrical insulator. An objective in lowering the loss tangent is creating a dielectric with a high insulation resistance. This study helped us understand better the relationship between loss tangent and reducing the oxygen vacancies by changing the temperature and pressure levels in the re-oxidation furnace.

References

1. Osburn, C. M., Kim, I., Han, S. K., "Vertically scaled MOSFET gate stacks and junctions: How far are we likely to go?" *IBM Journal of Research and Development,* 2002. **46**(2/3): pp. 299-315.

2. Wang, H.-.P., "Beyond the conventional transistor." *IBM Journal of Research and Development*, 2002. **46**(2/3): pp. 133-68.

3. Kishi, H., et al., "Base-Metal Electrode Multilayer Ceramic Capacitors: Past, Present and Future Perspectives." *Japan Journal of Applied Physics,* 2003. **42**: pp. 1-15.

4. Kahn, M., "Multilayer Ceramic Capacitors-Materials and Manufacture." *AVX Corporation Technical Information* Myrtle Beach, SC.

5. Cozzolino, M.J., and Ewell, G. J. "Failure Analysis of Surface- Mounted Capacitors." *Microelectronic Failure Analysis Desk Reference 2002 Supplement,* 2002.

6. Silvus, S., "Failure Analysis of Passive Components." *Microelectronic Failure Analysis Desk Reference 1999 Supplement,* 1999.

7. Madou, and L. Martens, "Electrical behavior of decoupling capacitors embedded in multi-layered PCBs." *IEEE Transactions on Electromagnetic Compatibility,* 2001. **43**(4): pp. 549-556.

8. L-S. Chen, S-L. Fu, and K-D. Huang, "Barium Titanate-Based Capacitors Buried Into Ceramic Substrates." *Jpn. J. Appl. Phys,* 1998. **37** (2): pp. L1241-L1243.

9. Kaiser, C., *The Capacitor Handbook.* 1993, New York, NY: Van Nostrand Reinhold.

10. Campbell, D. S. and Hayes, J. A., *Capacitive and Resistive Electronic Components.* 1994, Yverdon, Switzerland: Gordon & Breach Science Publishers. **8**.

11. Sinclair, I.R., *Passive Components: A User's Guide, 2nd Ed.* 1991, Oxford, England: Newnes

12. Parker, C.B. "Size Effects and Reliability of (Ba, Sr)TiO_3 Thin Films." *Ph.D. Dissertation North Carolina State University.* 2002

13. Ihlefeld, J. F., *et al.*, "Cu-Compatible Ultra-High Permittivity Dielectrics for Embedded Passive Components." *2003 Materials Research Society Symposium Proceedings.* 2004.

14. Burn, I. and Maher, G. H., "High Resistivity $BaTiO_3$ ceramics sintered in CO-CO_2 atmospheres." *Journal of Materials Science,* 1975. **10**: pp. 633-640.

15. Opitz, M.R., *et al.*, “Kinetic Process of Reoxidation of Base Metal Technology $BaTiO_3$ – Based Multilayer Capacitors.” *Journal of American Ceramic Society*, 2003. **86**(11): pp. 1879-84.

16. Loh, E., “A model of DC Leakage in ceramic capacitors.” *Journal of Applied Physics,* 1982. **53**(9): pp. 6229-35.

17. Schroeder, D.K., *Semiconductor Material and Device Characterization, 2nd Ed.* 1998, New York, NY: John Wiley.

18. Rawal, B.S. and Chan, N.H., “Conduction and Failure Mechanisms in Barium Titanate Based Ceramics Under Highly Accelerated Conditions.” *AVX Corporation Technical Information* Myrtle Beach, SC.

19. Waser, R., Baiatu, T., and Hardtl, K.-H., “DC Electrical Degradation of Perovskite-Type Titanates: I, Ceramics.” *Journal of American Ceramic Society,* 1990. **73**(6): pp. 1645-53.

20. Henderson, C., *Semiconductor Reliability Manual*. 2002.

21. Lehovec, K. and Shirn, G., “Conductivity Injection and Extraction in Polycrystalline Barium Titanate.” *Journal of Applied Physics,* 1962. **33**(6): pp. 2036-44.

22. Sall, J. Creighton, L. and Lehman, A., *JMP Start Statistics, 3rd Ed.* 2004, Victoria, Australia: Thomas.

23. Montgomery, D. C., *Design and Analysis of Experiments.* 2001, New York, NY: John Wiley.

24. Burn, I., “Ceramic Disk Capacitors with Base-Metal Electrodes.” *Ceramic Bulletin,* 1978. **57**(6): p. 600-604.

25. Smyth, D.M., *The Defect Chemistry of Metal Oxides.* 2000, New York, NY: Oxford Press.

26. *The Black Belt Memory Jogger*. 2002, Salem, NH: Six Sigma Academy.

27. Devore, J.L., *Probability and Statistics for Engineering and the Sciences, 5th Ed.* 2000, Pacific Grove, CA: Duxbury.

28. Shapiro, S.S., Wilk, M.B., and Chen, H.J., “A Comparative Study of Various Tests for Normality.” *Journal of the American Statistical Association,* 1968. 63: pp. 1343-1372

29. Website: www.statsoftinc.com/textbook/stnonpar

30. Daniel, W. W., *Applied Nonparametric Statistics.* 1978, Boston, MA: Houghton Mifflin Company.

31. Walpole, R.E., et al., *Probability and Statistics for Engineers and Scientists, 7th Ed.* 2002, Upper Saddle River, NJ: Prentice Hall.

32. JMP® Statistics and Graphics Guide. 2002, Cary, NC: SAS.

APPENDIX A:

MEASUREMENT SYSTEM ANALYSIS DATA

Operator	Sample	Trial	Conditions	Column #	Capacitor #	Capacitance(nF)	Loss Tan
Alisa	1	1	550, 1E-4	3	11	1.354	0.038
Alisa	2	1	450, 1E-5	2	8	0.922	0.034
Alisa	3	1	650, 1E-4	5	4	0.7	0.052
Alisa	4	1	450, 1E-3, #1	4	12	0.77	0.045
Alisa	5	1	450, 1E-3, #2	2	14	0.774	0.05
Alisa	6	1	650, 1E-5	6	11	0.946	0.028
Alisa	7	1	650, 1E-3	1	5	1.44	0.074
Alisa	8	1	450, 1E-4	3	3	1.253	0.034
Alisa	9	1	550, 1E-5	3	13	1.448	0.028
Alisa	10	1	550, 1E-3	4	3	1.483	0.027
Jon	1	1	650, 1E-4	5	4	1.043	0.076
Jon	2	1	550, 1E-4	3	11	1.33	0.032
Jon	3	1	650, 1E-5	6	11	0.944	0.028
Jon	4	1	650, 1E-3	1	5	1.428	0.072
Jon	5	1	450, 1E-3, #2	2	14	1.156	0.062
Jon	6	1	550, 1E-3	4	3	1.499	0.026
Jon	7	1	450, 1E-4	3	3	1.259	0.034
Jon	8	1	550, 1E-5	3	13	1.493	0.026
Jon	9	1	450, 1E-3, #1	4	12	1.18	0.052
Jon	10	1	450, 1E-5	2	8	0.917	0.034
Mark	1	1	650, 1E-5	6	11	0.94	0.035
Mark	2	1	550, 1E-5	3	13	1.491	0.031
Mark	3	1	450, 1E-4	3	3	0.888	0.034
Mark	4	1	450, 1E-5	2	8	1.054	0.034
Mark	5	1	550, 1E-4	3	11	0.797	0.028
Mark	6	1	550, 1E-3	4	3	1.038	0.034
Mark	7	1	650, 1E-3	1	5	1.44	0.077
Mark	8	1	450, 1E-3, #2	2	14	0.7	0.052
Mark	9	1	450, 1E-3, #1	4	12	1.172	0.053
Mark	10	1	650, 1E-4	5	4	0.706	0.062
Alisa	1	2	550, 1E-5	3	13	1.474	0.027
Alisa	2	2	450, 1E-3, #1	4	12	1.212	0.053
Alisa	3	2	650, 1E-3	1	5	1.424	0.071
Alisa	4	2	450, 1E-5	2	8	1.495	0.04
Alisa	5	2	450, 1E-3, #2	2	14	1.126	0.056
Alisa	6	2	650, 1E-4	5	4	1.035	0.079
Alisa	7	2	650, 1E-5	6	11	0.949	0.036
Alisa	8	2	450, 1E-4	3	3	1.268	0.035
Alisa	9	2	550, 1E-4	3	11	1.329	0.035
Alisa	10	2	550, 1E-3	4	3	1.499	0.027

Operator	Sample	Trial	Conditions	Column #	Capacitor #	Capacitance(nF)	Loss Tan
Jon	1	2	450, 1E-4	3	3	1.261	0.035
Jon	2	2	450, 1E-3, #1	4	12	1.224	0.054
Jon	3	2	650, 1E-4	5	4	0.702	0.063
Jon	4	2	450, 1E-5	2	8	0.922	0.034
Jon	5	2	550, 1E-5	3	13	1.471	0.026
Jon	6	2	650, 1E-5	6	11	0.948	0.028
Jon	7	2	450, 1E-3, #2	2	14	1.137	0.057
Jon	8	2	550, 1E-4	3	11	1.35	0.037
Jon	9	2	550, 1E-3	4	3	1.51	0.028
Jon	10	2	650, 1E-3	1	5	1.428	0.071
Mark	1	2	550, 1E-3	4	3	1.482	0.03
Mark	2	2	650, 1E-3	1	5	1.422	0.075
Mark	3	2	450, 1E-4	3	3	0.898	0.032
Mark	4	2	450, 1E-5	2	8	1.533	0.037
Mark	5	2	650, 1E-4	5	4	1.031	0.08
Mark	6	2	450, 1E-3, #1	4	12	0.787	0.045
Mark	7	2	550, 1E-4	3	11	1.335	0.036
Mark	8	2	650, 1E-5	6	11	0.949	0.027
Mark	9	2	450, 1E-3, #2	2	14	1.135	0.055
Mark	10	2	550, 1E-5	3	13	1.485	0.028

APPENDIX B:
RAW DATA FROM 3^2 AND 2^2 EXPERIMENTS

Data From 3^2 Experiment

Temperature			450 (°C)	
Pressure			10^{-3} Torr	
Sample	Row	Capacitance (nF)	Loss Tan	Order
1	2	1.12	0.065	3
2	2	1.14	0.066	4
3	2	1.129	0.061	5
4	2	1.41	0.046	6
5	2	1.146	0.044	7
6	2	1.07	0.043	8
7	2	1.158	0.08	9
8	2	1.261	0.039	10
9	2	1.22	0.041	11
10	2	1.221	0.037	12
11	3	1.229	0.045	9
12	3	1.245	0.044	8
13	3	1.263	0.037	7
14	3	1.167	0.044	6
15	3	1.152	0.045	5
16	3	1.203	0.048	4
17	3	1.223	0.053	3
18	3	1.21	0.06	2
19	3	1.123	0.057	1
20	4	2.11	0.0598	1
21	4	2.198	0.0571	2
22	4	1.078	0.057	3
23	4	1.157	0.058	4
24	4	1.3	0.048	5
25	4	1.301	0.046	6
26	4	1.276	0.045	7
27	4	1.279	0.044	8
28	4	1.211	0.051	9
29	4	1.239	0.051	10
30	5	1.185	0.068	9
31	5	1.205	0.063	8
32	5	1.243	0.067	7
33	5	1.235	0.055	6
34	5	1.201	0.056	5
35	5	1.193	0.063	4
36	5	1.176	0.058	3
37	5	1.071	0.07	2
38	5	1.182	0.066	1
39	1	1.125	0.048	1
40	1	1.133	0.044	2

Temperature			450 (°C)	
Pressure			10^{-4} Torr	
Sample	Row	Capacitance (nF)	Loss Tan	Order
1	1	1.569	0.054	1
2	1	1.57	0.054	2
3	1	1.748	0.047	3
4	1	1.524	0.054	4
6	1	1.372	0.06	6
7	1	1.343	0.06	7
8	1	1.42	0.06	8
10	2	1.352	0.051	9
11	2	1.504	0.046	8
12	2	1.475	0.052	7
13	2	1.432	0.059	6
14	2	1.52	0.06	5
15	2	1.45	0.069	4
16	2	1.301	0.081	3
17	2	1.241	0.092	2
19	3	1.255	0.072	1
20	3	1.333	0.057	2
21	3	1.476	0.044	3
22	3	1.482	0.045	4
23	3	1.613	0.037	5
24	3	1.639	0.037	6
25	3	1.532	0.034	7
26	3	1.534	0.033	8
27	3	1.533	0.032	9
28	3	1.556	0.032	10
29	4	1.442	0.024	6
30	4	1.61	0.026	5
31	4	1.514	0.026	4
32	4	1.63	0.027	3
33	4	1.564	0.026	2
34	4	1.482	0.026	1
35	5	1.669	0.026	1
36	5	1.668	0.024	2
37	5	1.574	0.023	3
38	5	1.531	0.023	4
39	5	1.607	0.024	5
40	5	1.635	0.024	6

Temperature			450 (°C)	
Pressure			10^{-5} Torr	
Sample	Row	Capacitance (nF)	Loss Tan	Order
1	1	1.495	0.04	1
2	1	1.433	0.031	2
3	1	1.56	0.028	3
4	1	1.523	0.028	4
5	1	1.426	0.027	5
6	1	1.405	0.025	6
7	1	1.493	0.027	7
8	1	1.388	0.024	8
9	2	1.42	0.025	8
10	2	1.598	0.029	7
11	2	1.587	0.029	6
12	2	1.659	0.03	5
13	2	1.573	0.027	4
14	2	1.569	0.033	3
15	2	1.476	0.042	2
16	2	1.377	0.045	1
17	3	1.392	0.058	1
18	3	1.081	0.054	2
19	3	1.245	0.053	3
20	3	1.242	0.053	4
21	3	1.585	0.037	5
22	3	1.557	0.033	6
23	3	1.453	0.031	7
24	3	1.646	0.032	8
25	3	1.535	0.028	9
26	4	1.483	0.037	8
27	4	1.619	0.035	7
28	4	1.517	0.039	6
29	4	1.464	0.043	5
30	4	1.472	0.045	4
31	4	1.457	0.048	3
32	4	1.438	0.054	2
34	5	1.388	0.052	1
35	5	1.433	0.048	2
36	5	1.51	0.045	3
37	5	1.378	0.044	4
38	5	1.472	0.039	5
39	5	1.519	0.042	6
40	5	1.393	0.054	1

Temperature			550(°C)	
Pressure			10^{-3} Torr	
Sample	Row	Capacitance (nF)	Loss Tan	Order
1	1	1.152	0.026	1
2	1	1.242	0.023	2
3	1	1.188	0.029	3
4	1	1.193	0.027	4
5	1	1.194	0.028	5
6	1	1.285	0.027	6
8	1	1.283	0.023	8
9	1	1.253	0.025	9
10	2	1.348	0.025	9
11	2	1.272	0.027	8
12	2	1.235	0.029	7
13	2	1.264	0.028	6
14	2	1.325	0.026	5
15	2	1.225	0.027	4
16	2	1.283	0.027	3
17	2	1.206	0.03	2
18	2	1.214	0.029	1
19	3	1.325	0.025	1
20	3	1.28	0.026	2
21	3	1.348	0.026	3
22	3	1.18	0.027	4
23	3	1.145	0.032	5
24	3	1.234	0.032	6
25	3	1.228	0.03	7
26	3	1.373	0.029	8
27	3	1.326	0.025	9
28	3	1.449	0.027	10
29	3	1.388	0.023	11
31	4	1.442	0.025	10
32	4	1.312	0.027	9
33	4	1.211	0.03	8
34	4	1.189	0.029	7
35	4	1.274	0.031	6
36	4	1.195	0.029	5
37	4	1.068	0.031	4
38	4	1.113	0.032	3
39	4	1.079	0.034	2
40	4	1.138	0.04	1

Temperature			550(°C)	
Pressure			10^{-4} Torr	
Sample	Row	Capacitance (nF)	Loss Tan	Order
2	2	1.213	0.028	2
3	2	1.25	0.043	3
4	2	1.236	0.027	4
5	2	1.245	0.026	5
6	2	1.295	0.028	6
7	2	1.16	0.026	7
8	2	1.266	0.026	8
9	2	1.284	0.026	9
10	2	1.341	0.024	10
11	3	1.282	0.028	9
12	3	1.252	0.027	8
13	3	1.263	0.03	7
14	3	1.232	0.028	6
15	3	1.304	0.03	5
16	3	1.237	0.027	4
17	3	1.227	0.026	3
18	3	1.205	0.027	2
19	3	1.217	0.026	1
20	4	1.252	0.037	1
21	4	1.34	0.034	2
22	4	1.301	0.036	3
23	4	1.239	0.038	4
24	4	1.312	0.058	5
25	4	1.223	0.038	6
26	4	1.218	0.04	7
27	4	1.255	0.043	8
40	4	1.21	0.043	9

Temperature			550(°C)	
Pressure			10^{-5} Torr	
Sample	Row	Capacitance (nF)	Loss Tan	Order
1	1	1.396	0.026	1
2	1	1.378	0.026	2
3	1	1.403	0.026	3
4	1	1.439	0.026	4
5	1	1.426	0.026	5
6	1	1.413	0.026	6
7	1	1.311	0.023	7
8	1	1.291	0.025	8
9	2	1.183	0.037	8
10	2	1.253	0.026	7
11	2	0.9	0.021	6
12	2	1.446	0.027	5
13	2	1.39	0.025	4
14	2	1.4	0.025	3
15	2	1.475	0.028	2
16	2	1.434	0.027	1
17	3	1.437	0.028	1
18	3	1.384	0.029	2
19	3	1.354	0.028	3
20	3	1.344	0.029	4
21	3	1.338	0.03	5
22	3	1.29	0.028	6
23	3	1.281	0.031	7
24	3	1.33	0.029	8
25	3	1.416	0.036	9
26	4	1.366	0.028	8
27	4	1.402	0.028	7
28	4	1.425	0.028	6
29	4	1.451	0.027	5
30	4	1.422	0.028	4
31	4	1.408	0.029	3
32	4	1.437	0.027	2
33	4	1.456	0.026	1
34	5	1.368	0.025	1
35	5	1.412	0.028	2
36	5	1.41	0.027	3
37	5	1.408	0.028	4
38	5	1.499	0.029	5
39	5	1.366	0.028	6
40	5	1.363	0.026	7

Temperature			650(°C)	
Pressure			10^{-3} Torr	
Sample	Row	Capacitance (nF)	Loss Tan	Order
1	1	1.218	0.039	1
2	1	1.261	0.035	2
3	1	1.264	0.038	3
4	1	1.253	0.035	4
5	1	1.334	0.036	5
6	1	1.261	0.035	6
7	1	1.298	0.037	7
8	1	1.266	0.037	8
9	1	1.281	0.038	9
10	2	1.388	0.036	12
11	2	1.296	0.038	11
12	2	1.31	0.038	10
13	2	1.288	0.037	9
14	2	1.296	0.035	8
15	2	1.292	0.035	7
16	2	1.304	0.037	6
17	2	1.381	0.039	5
18	2	1.417	0.039	4
19	2	1.231	0.036	3
20	2	1.212	0.038	2
21	2	1.233	0.037	1
22	4	1.223	0.033	1
23	4	1.24	0.036	2
24	4	1.286	0.041	3
25	4	1.268	0.04	4
26	4	1.281	0.04	5
27	4	1.22	0.037	6
28	4	1.293	0.038	7
29	4	1.31	0.038	8
30	4	1.303	0.038	9
31	4	1.289	0.037	10
32	4	1.354	0.039	11
33	4	1.341	0.045	12
34	4	1.304	0.042	13
35	5	1.313	0.058	11
36	5	1.354	0.06	10
37	5	1.37	0.052	9
38	5	1.365	0.054	8
39	5	1.318	0.058	7
40	5	1.304	0.056	6

Temperature			650(°C)	
Pressure			10^{-4} Torr	
Sample	Row	Capacitance (nF)	Loss Tan	Order
10	2	0.98	0.09	9
11	2	0.888	0.087	8
13	2	0.909	0.093	5
14	2	0.892	0.09	4
17	3	0.981	0.075	1
18	3	0.887	0.064	2
19	3	0.893	0.059	3
20	3	0.895	0.051	4
21	4	0.943	0.072	5
22	4	0.965	0.049	6
23	4	0.93	0.042	7
24	4	1.045	0.051	8
25	4	1.052	0.051	9
26	4	1.029	0.05	10
27	4	1.029	0.08	11
28	5	1.043	0.067	14
29	5	1.045	0.07	12
30	5	1.037	0.063	11
31	5	0.995	0.049	10
32	5	1.021	0.047	9
33	5	1.033	0.047	8
34	5	0.901	0.045	7
35	5	0.941	0.04	6
36	5	1.036	0.053	4
38	5	1.048	0.057	2

Temperature			650(°C)	
Pressure			10^{-5} Torr	
Sample	Row	Capacitance (nF)	Loss Tan	Order
2	2	0.934	0.067	2
3	2	0.896	0.044	3
4	2	0.821	0.034	4
5	2	0.822	0.037	5
6	2	0.833	0.039	6
7	2	0.921	0.036	7
8	2	0.911	0.03	8
9	2	0.927	0.03	9
10	2	0.929	0.03	10
11	2	0.857	0.027	11
12	3	0.924	0.029	14
13	3	0.866	0.026	13
14	3	0.823	0.027	12
15	3	0.892	0.029	11
16	3	0.928	0.03	10
17	3	0.958	0.031	9
18	3	0.874	0.031	8
19	3	0.886	0.031	7
20	3	0.904	0.032	6
21	3	0.867	0.033	5
22	3	0.921	0.031	4
23	3	0.912	0.051	3
24	3	0.929	0.064	2
26	4	0.929	0.049	2
27	4	0.974	0.044	3
28	4	0.951	0.032	4
29	4	0.867	0.032	5
30	4	0.919	0.031	6
31	4	0.861	0.031	7
32	4	0.97	0.03	8
33	4	0.929	0.031	9
34	4	0.873	0.03	10
35	4	0.911	0.028	11
36	4	0.915	0.028	12
37	4	0.824	0.026	13
38	5	0.908	0.026	13
39	5	0.885	0.028	12
40	5	0.863	0.031	11

Data From 2^2 Experiment

ANNEAL 1			
Film Position			1
Temperature			600
Pressure			2*10^-5
	Column	**Row**	**Loss Tan**
1	4	15	0.1025
4	4	11	0.0873
6	6	13	0.1028
7	2	18	0.0901
8	2	10	0.0698
9	2	16	0.0872
10	3	8	0.0652
11	2	15	0.0878
12	6	14	0.0996
13	5	6	0.074
14	3	15	0.0896
15	6	8	0.0827
16	3	14	0.0863
17	2	14	0.0825
18	2	17	0.0876
19	3	5	0.0933
20	1	10	0.0667
22	2	9	0.059
23	6	11	0.0874
24	3	16	0.1004
25	6	17	0.0939
26	5	16	0.0835
27	5	14	0.088
28	1	7	0.0962
29	4	8	0.059
30	3	9	0.0572
31	6	9	0.0848
32	6	5	0.1062
33	2	11	0.0626
34	6	10	0.0935
35	6	15	0.0875
36	6	12	0.0992
37	3	6	0.05
38	4	12	0.0846
39	1	15	0.0654
40	4	9	0.063

ANNEAL 1			
Film Position			2
Temperature			500
Pressure			5*10^-6
	Column	**Row**	**Loss Tan**
1	4	0	0.082
2	2	11	0.102
3	6	9	0.14
4	4	3	0.119
6	4	5	0.1246
8	2	12	0.104
10	2	5	0.1049
11	4	16	0.132
12	6	4	0.109
14	3	17	0.095
15	2	8	0.0993
17	6	1	0.087
18	3	11	0.1285
19	5	18	0.123
20	2	18	0.097
21	2	3	0.085
22	6	8	0.134
23	2	14	0.0983
24	5	0	0.072
25	5	10	0.152
26	4	11	0.1194
27	5	8	0.1232
28	3	2	0.166
29	6	2	0.088
30	6	14	0.129
32	4	1	0.093
33	5	11	0.137
34	3	13	0.0953
35	5	12	0.133
36	4	18	0.106
37	3	8	0.0959
38	6	3	0.096
39	4	7	0.1177
40	4	4	0.1068

ANNEAL 1			
Film Position			3
Temperature			600
Pressure			5*10^-6
	Row	Column	Loss Tan
1	5	3	0.118
2	3	9	0.1085
3	5	13	0.1223
4	2	7	0.0807
5	4	4	0.114
6	3	2	0.073
7	6	16	0.09
8	5	17	0.092
9	6	11	0.1198
10	4	15	0.1199
11	2	9	0.0751
12	3	14	0.1086
13	2	2	0.053
14	4	16	0.103
15	4	7	0.1165
16	3	4	0.097
17	6	13	0.126
18	6	10	0.116
19	4	18	0.084
20	5	16	0.1109
21	3	16	0.0991
22	5	5	0.116
23	2	14	0.0895
24	6	14	0.113
25	4	2	0.103
26	5	18	0.081
27	6	3	0.102
28	3	11	0.1121
29	3	8	0.107
30	2	10	0.0815
31	2	5	0.0629
32	5	1	0.073
33	2	8	0.0836
34	5	12	0.1258
35	5	11	0.1276
36	6	9	0.1131
38	2	15	0.0852
39	6	15	0.109
40	2	4	0.111

ANNEAL 1			
Film Position			4
Temperature			500
Pressure			2*10^-5
	Row	Column	Loss Tan
2	2	17	0.059
3	2	4	0.094
4	1	2	0.1
5	3	4	0.104
6	3	6	0.087
7	4	5	0.124
8	5	8	0.141
9	6	6	0.136
10	4	2	0.122
12	2	12	0.064
13	5	5	0.125
14	4	8	0.149
15	4	6	0.124
16	4	11	0.129
17	3	12	0.075
18	1	8	0.079
19	3	14	0.123
20	4	15	0.14
21	4	9	0.107
22	1	3	0.063
23	6	12	0.143
24	1	7	0.078
25	2	9	0.083
26	2	16	0.103
27	3	3	0.118
28	4	10	0.116
29	1	5	0.07
31	3	10	0.0772
32	4	12	0.098
33	4	13	0.144
34	2	1	0.087
35	5	12	0.122
36	4	7	0.131
37	3	5	0.101
38	1	10	0.08
39	5	11	0.137
40	4	4	0.121

ANNEAL 1			
Film Position			2
Temperature			550
Pressure			10^-5
	Column	**Row**	**Loss Tan**
1	3	1	0.0589
2	2	1	0.0468
3	2	15	0.055
4	1	11	0.0655
5	5	14	0.0411
6	3	4	0.0527
7	2	12	0.0525
8	4	6	0.045
9	2	11	0.0573
10	4	7	0.0435
11	2	6	0.052
12	4	17	0.0461
13	5	4	0.0433
14	1	6	0.0529
15	2	2	0.0462
16	3	16	0.0499
17	5	15	0.0389
18	3	17	0.053
19	4	18	0.0428
20	5	11	0.0395
21	2	5	0.0509
22	1	13	0.0541
23	3	3	0.0484
24	3	8	0.0474
25	2	8	0.0515
26	1	17	0.0551
27	3	7	0.0494
28	3	5	0.0504
29	2	4	0.0509
30	5	18	0.045
31	2	16	0.0569
32	2	2	0.047
33	3	9	0.0473
34	3	13	0.0493
35	2	12	0.0489
36	1	14	0.0657
37	5	10	0.0437
38	1	12	0.0583
39	2	14	0.0517
40	5	12	0.0385

ANNEAL 2			
Film Position			1
Temperature			500
Pressure			2*10^-5
	Column	Row	Loss Tan
1	3	11	0.15
2	3	15	0.115
3	1	12	0.126
4	6	14	0.099
5	6	15	0.098
6	5	2	0.095
7	2	18	0.119
8	6	5	0.088
9	6	10	0.098
10	5	14	0.126
11	5	6	0.126
12	4	10	0.15
13	5	17	0.062
14	1	8	0.143
15	3	10	0.155
16	1	9	0.154
17	2	4	0.114
18	2	17	0.142
19	1	17	0.12
20	1	4	0.119
21	5	18	0.058
22	2	15	0.132
23	5	7	0.115
24	4	12	0.166
25	6	9	0.095
26	6	7	0.101
27	3	7	0.155
28	6	8	0.0964
29	4	15	0.113
30	1	14	0.116
31	3	8	0.147
32	3	14	0.142
34	6	13	0.089
35	1	10	0.142
36	3	2	0.125
37	3	17	0.129
38	6	12	0.096
39	5	9	0.159
40	4	5	0.131

ANNEAL 2			
Film Position			2
Temperature			600
Pressure			5*10^-6
	Column	Row	Loss Tan
1	1	5	0.131
3	2	11	0.129
4	4	12	0.1152
5	5	11	0.0801
6	3	12	0.131
7	4	1	0.123
8	3	3	0.127
9	6	2	0.123
10	1	12	0.135
11	4	14	0.1029
12	2	2	0.105
13	5	1	0.072
14	2	3	0.127
15	4	6	0.122
16	5	9	0.0775
17	2	7	0.152
18	5	10	0.0757
19	6	4	0.114
20	6	3	0.123
21	6	8	0.0893
22	1	10	0.142
23	5	5	0.0796
24	4	2	0.125
25	5	4	0.0756
26	1	7	0.138
27	4	15	0.099
28	5	15	0.0738
29	2	13	0.141
30	6	15	0.088
31	2	17	0.132
32	5	13	0.0805
33	4	3	0.126
34	6	5	0.113
35	2	6	0.151
36	2	14	0.139
37	5	12	0.0806
38	4	13	0.106
39	4	18	0.11
40	6	6	0.115

ANNEAL 2			
Film Position			3
Temperature			600
Pressure			2*10^-5
	Column	Row	Loss Tan
1	2	11	0.1224
2	3	4	0.1279
3	4	7	0.119
4	5	15	0.102
5	3	8	0.127
6	3	10	0.1383
7	2	2	0.112
8	5	4	0.102
9	4	15	0.115
10	4	17	0.117
11	3	13	0.1096
12	5	1	0.067
13	5	14	0.11
14	4	14	0.118
15	5	17	0.092
16	4	4	0.092
17	5	10	0.091
18	5	11	0.113
19	3	2	0.109
20	1	3	0.11
21	5	13	0.115
22	2	15	0.12
23	2	1	0.1
24	5	16	0.101
25	4	2	0.087
26	5	18	0.093
27	3	6	0.103
28	3	14	0.125
29	3	17	0.108
30	6	10	0.104
31	3	5	0.116
32	2	8	0.128
33	1	14	0.107
34	1	15	0.116
35	4	18	0.105
36	4	13	0.129
37	1	12	0.115
38	3	16	0.113
39	5	7	0.086
40	6	9	0.068

ANNEAL 2			
Film Position			4
Temperature			500
Pressure			5*10^-6
	Column	Row	Loss Tan
1	3	14	0.176
2	5	7	0.163
3	5	16	0.175
4	5	10	0.165
5	5	15	0.147
6	6	2	0.11
7	5	9	0.161
8	2	9	0.14
9	6	4	0.11
10	6	12	0.178
11	5	4	0.135
12	3	1	0.122
13	4	14	0.174
14	2	7	0.146
15	4	12	0.173
16	6	11	0.171
17	6	7	0.125
18	5	3	0.127
19	4	10	0.146
20	6	13	0.18
21	3	6	0.148
22	4	3	0.13
23	6	8	0.144
24	3	10	0.177
25	3	13	0.171
26	6	9	0.154
27	3	9	0.146
28	4	11	0.145
29	2	3	0.135
30	3	16	0.143
31	4	4	0.132
32	2	5	0.142
33	3	11	0.169
34	5	11	0.167
35	3	2	0.119
36	3	15	0.161
37	5	2	0.113
38	6	10	0.162
39	5	8	0.161
40	2	6	0.133

ANNEAL 2			
Film Position			3
Temperature			550
Pressure			10^-5
	Column	**Row**	**Loss Tan**
1	3	15	0.0416
2	2	5	0.0482
3	5	3	0.0341
4	4	11	0.0548
5	4	3	0.0385
6	1	13	0.0521
7	4	17	0.0499
8	5	16	0.0488
9	5	10	0.0407
10	1	8	0.059
11	3	5	0.0498
12	4	2	0.0454
13	3	1	0.069
14	6	8	0.0308
15	2	9	0.0396
16	4	6	0.0397
17	6	4	0.0302
18	5	8	0.0403
19	5	17	0.0484
20	6	2	0.0316
21	4	5	0.0381
22	3	10	0.0483
23	6	12	0.0314
24	5	15	0.0469
25	2	4	0.05
26	1	12	0.0507
27	3	14	0.0419
29	4	14	0.059
30	6	15	0.0299
31	4	16	0.062
32	5	2	0.033
33	3	11	0.0415
34	6	11	0.0302
35	5	13	0.0482
36	4	12	0.0559
37	2	6	0.0437
38	5	4	0.0325
39	5	11	0.0461
40	3	8	0.0553

APPENDIX C:

NORMAL FITS FOR 2^2 EXPERIMENTS

Anneal 1

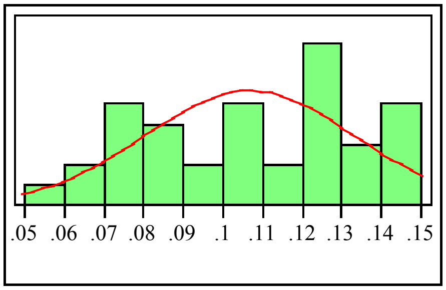

Fitted Normal Distribution for Loss Tangent at 500°C/2x10^{-5} Torr

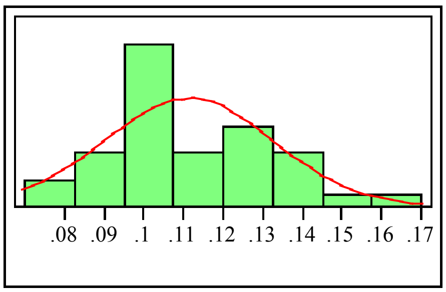

Fitted Normal Distribution for Loss Tangent at 500°C/5x10^{-6} Torr

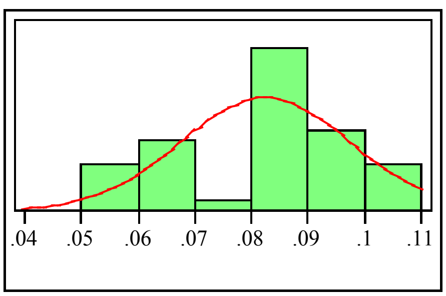

Fitted Normal Distribution for Loss Tangent at 600°C/2x10^{-5} Torr

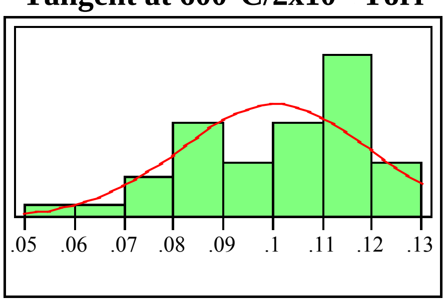

Fitted Normal Distribution for Loss Tangent at 600°C/5x10^{-6} Torr

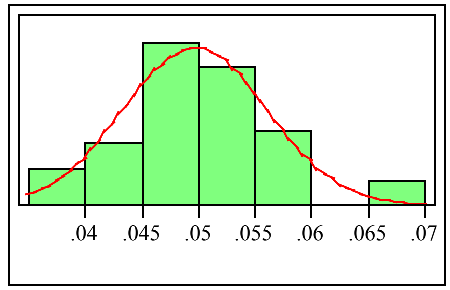

Fitted Normal Distribution for Loss Tangent at 550°C/10^{-5} Torr

Anneal 2

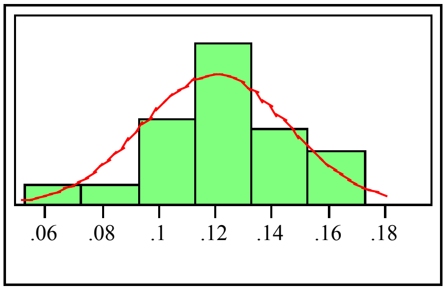

Fitted Normal Distribution for Loss Tangent at 500°C/2x10^{-5} Torr

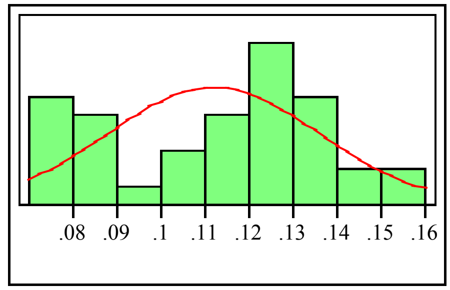

Fitted Normal Distribution for Loss Tangent at 550°C/10^{-5} Torr

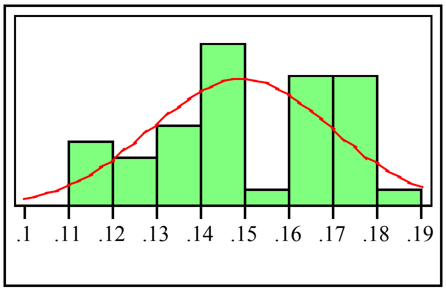

Fitted Normal Distribution for Loss Tangent at 500°C/5x10^{-6} Torr

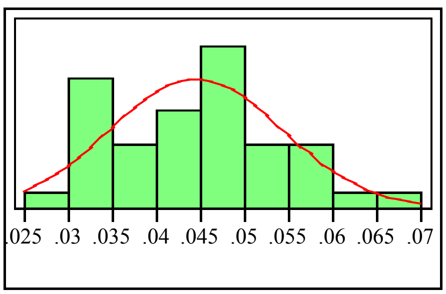

Fitted Normal Distribution for Loss Tangent at 600°C/2x10^{-5} Torr

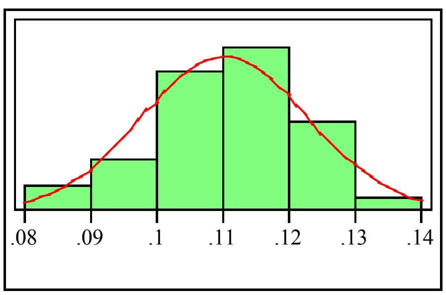

Fitted Normal Distribution for Loss Tangent at 600°C/5x10^{-6} Torr